PRODUCTION OF BIODEGRADABLE UV PROTECTION FILM USING CELLULOSE AND
LIGNIN EXTRACTED FROM OIL PALM EMPTY FRUIT BUNCH

Mr. Muhammad Taufiq Haqiqi

จุฬาลงกรณ์มหาวิทยาลัย
CHULALONGKORN UNIVERSITY

A Thesis Submitted in Partial Fulfillment of the Requirements
for the Degree of Master of Science in Biotechnology
Common Course
FACULTY OF SCIENCE
Chulalongkorn University
Academic Year 2020

การผลิตฟิล์มป้องกันยูวีย่อยสลายทางชีวภาพได้โดยใช้เซลลูโลสและลิกนินที่สกัดจากเศษทะลาย
ปาล์มน้ำมัน

นายมูฮัมหมัด เทาฟีค ฮาคีคี

วิทยานิพนธ์นี้เป็นส่วนหนึ่งของการศึกษาตามหลักสูตรปริญญาวิทยาศาสตรมหาบัณฑิต
สาขาวิชาเทคโนโลยีชีวภาพ ไม่สังกัดภาควิชา/เทียบเท่า
คณะวิทยาศาสตร์ จุฬาลงกรณ์มหาวิทยาลัย
ปีการศึกษา 2563
ลิขสิทธิ์ของจุฬาลงกรณ์มหาวิทยาลัย

Thesis Title	PRODUCTION OF BIODEGRADABLE UV PROTECTION FILM USING CELLULOSE AND LIGNIN EXTRACTED FROM OIL PALM EMPTY FRUIT BUNCH
By	Mr. Muhammad Taufiq Haqiqi
Field of Study	Biotechnology
Thesis Advisor	Associate Professor SEHANAT PRASONGSUK, Ph.D.
Thesis Co Advisor	Associate Professor PONGTHARIN LOTRAKUL, Ph.D. PRASIT PATTANANUWAT, Ph.D.

Accepted by the FACULTY OF SCIENCE, Chulalongkorn University in Partial Fulfillment of the Requirement for the Master of Science

.... Dean of the FACULTY OF SCIENCE
(Professor POLKIT SANGVANICH, Ph.D.)

THESIS COMMITTEE

.... Chairman
(Assistant Professor JITTRA PIAPUKIEW, Ph.D.)

.... Thesis Advisor
(Associate Professor SEHANAT PRASONGSUK, Ph.D.)

.... Thesis Co-Advisor
(Associate Professor PONGTHARIN LOTRAKUL, Ph.D.)

.... Thesis Co-Advisor
(PRASIT PATTANANUWAT, Ph.D.)

.... Examiner
(SUPAWIN WATCHARAMUL, Ph.D.)

.... Examiner
(WICHANEE BANKEEREE, Ph.D.)

.... External Examiner
(Professor Rudianto Amirta, Ph.D.)

มูฮัมหมัด เทาฟีค ฮาคีคี : การผลิตฟิล์มป้องกันยูวีย่อยสลายทางชีวภาพได้โดยใช้เซลลูโลสและลิกนินที่สกัดจากเศษทะลายปาล์มน้ำมัน. (PRODUCTION OF BIODEGRADABLE UV PROTECTION FILM USING CELLULOSE AND LIGNIN EXTRACTED FROM OIL PALM EMPTY FRUIT BUNCH) อ.ที่ปรึกษาหลัก : สีหนาท ประสงค์สุข, อ.ที่ปรึกษาร่วม : พงศ์ธาริน โล่ห์ตระกูล,ประสิทธิ์ พัฒนะนุวัฒน์

กระบวนการที่เหมาะสมในการสกัดเซลลูโลสจากทะลายเปล่า (empty fruit bunch, EFB) ของปาล์มน้ำมัน ประกอบด้วยการปรับสภาพด้วยกรด (H_2SO_4 ร้อยละ 0.5 โดยปริมาตร) การสกัดด้วยด่าง (NaOH ร้อยละ 15 โดยน้ำหนัก) และการฟอกขาวปราศจากคลอรีน (H_2O_2 ร้อยละ 10 โดยน้ำหนักต่อปริมาตร) พบว่าให้เยื่อที่มีปริมาณเซลลูโลสสูงที่สุด เท่ากับร้อยละ 83.42 กระบวนการเอสเตอร์ริฟิเคชันของ EFB เซลลูโลส ไปเป็นคาร์บอกซิเมทิลเซลลูโลส (carboxymethyl cellulose, CMC) ที่ละลายน้ำได้ดีขึ้น (ร้อยละ 81.32) นำ EFB CMC (ร้อยละ 2.5 โดยน้ำหนักต่อปริมาตร) มาผสมกับกลีเซอรอล (ร้อยละ 0.5 โดยน้ำหนักต่อปริมาตร) เพื่อผลิตคอมโพสิตฟิล์มโดยวิธีการขึ้นรูปจากสารละลาย ลิกนินที่ได้จากการตกตะกอนด้วยกรดของน้ำดำของ EFB จะถูกนำมาใช้ในฟิล์มที่ความเข้มข้นที่แตกต่างกัน และตรวจสอบผลที่มีต่อสมบัติการป้องกันยูวีของฟิล์ม จากการทดลองพบว่า ฟิล์มที่ปราศจากการเติมลิกนินสามารถปิดกั้นการผ่านของรังสียูวีบี (UV-B) ได้อย่างสมบูรณ์ การเติมลิกนินทุกความเข้มข้นช่วยเพิ่มการป้องกันรังสี ยูวีเอ (UV-A) และสมบัติทางกายภาพอื่น ๆ ของฟิล์ม เช่น ความหยาบของพื้นผิว ความหนา และความเสถียรทางความร้อน ให้ดีขึ้นได้อย่างมีนัยสำคัญ แต่ไม่มีผลอย่างมีนัยสำคัญต่อความสามารถในการซึมผ่านของไอน้ำและความทนต่อแรงดึง EFB CMC ฟิล์มที่เพิ่มปริมาณลิกนิน ร้อยละ 0.2 โดยน้ำหนักต่อปริมาตร เป็นองค์ประกอบที่เหมาะสมเนื่องจากมีความสามารถในการป้องกันยูวีเอและยูวีบีอย่างสมบูรณ์ มีการต้านอนุมูลอิสระที่สูงที่สุดและมีประสิทธิภาพเชิงกลที่ดี

สาขาวิชา เทคโนโลยีชีวภาพ	ลายมือชื่อนิสิต ....
ปีการศึกษา 2563	ลายมือชื่อ อ.ที่ปรึกษาหลัก ....
	ลายมือชื่อ อ.ที่ปรึกษาร่วม ....
	ลายมือชื่อ อ.ที่ปรึกษาร่วม ....

6172186723 : MAJOR BIOTECHNOLOGY

KEYWORD: Carboxymethyl cellulose, Empty fruit bunch, Lignin, UV protection

Muhammad Taufiq Haqiqi : PRODUCTION OF BIODEGRADABLE UV PROTECTION FILM USING CELLULOSE AND LIGNIN EXTRACTED FROM OIL PALM EMPTY FRUIT BUNCH. Advisor: Assoc. Prof. SEHANAT PRASONGSUK, Ph.D. Co-advisor: Assoc. Prof. PONGTHARIN LOTRAKUL, Ph.D., PRASIT PATTANANUWAT, Ph.D.

The optimized process for cellulose extraction from oil palm empty fruit bunch (EFB) consisting of acid pretreatment (0.5% (v/v) H_2SO_4), alkaline extraction (15% (w/w) NaOH), and chlorine-free bleaching (10% (w/v) H_2O_2) yielded pulp with the highest cellulose content at 83.42%. The EFB cellulose was then etherified into carboxymethyl cellulose (CMC) which was readily water-soluble (81.32%). The EFB CMC (2.5% (w/v)) was blended with glycerol (0.5 % (w/v)) to produce a composite film by a solution casting method. Lignin obtained from acid precipitation of the EFB black liquor was added into the film at different concentrations, and its influence on the UV-protection property was evaluated. Interestingly, the film without lignin incorporation completely blocked UV-B transmittance. The addition of lignin at all concentrations significantly improved the UV-A blocking and other physical properties, such as the surface roughness, thickness, and thermal stability, although the water vapor permeability and tensile strength were not significantly affected. The EFB CMC film supplemented with 0.2% (w/v) lignin was observed to be the optimized composition according to its total UV-A and UV-B protection capacity, highest antioxidant activity, and preferable mechanical performance.

Field of Study: Biotechnology	Student's Signature ....
Academic Year: 2020	Advisor's Signature ....
	Co-advisor's Signature ....
	Co-advisor's Signature ....

v

ACKNOWLEDGEMENTS

TABLE OF CONTENTS

Page

จุฬาลงกรณ์มหาวิทยาลัย

CHULALONGKORN UNIVERSITY

LIST OF TABLES

LIST OF FIGURES

CHAPTER I

INTRODUCTION

1.1 Rationale

Nowadays, severe environmental problems have escalated partly due to a rapid increase in plastic waste contamination, especially in the terrestrial and aquatic ecosystems (Sigler, 2014). On land, the burning of municipal solid wastes (MSW) containing plastic in the open field releases harmful gases such as dioxins, furans, mercury, and polychlorinated biphenyl compounds, adversely affecting the health of humans and animals (Verma et al., 2016). Most plastic wastes take hundreds of years to naturally degrade under ambient conditions; thus, they are rapidly accumulated in nature (Singh et al., 2017). Among the currently produced plastic products, the flexible plastic film is one of the most manufactured customized into various merchandises, mostly disposable ones (Horodytska et al., 2018). The single-use and short-term utilization of plastic films are believed to be a major reason for more and more plastic waste accumulation every year.

One of the most commercial plastic film products is a UV protection film widely used in buildings and cars. It is made from polyethylene terephthalate (PET) containing inorganic metal oxide nanoparticles. The global production of PET film has been estimated at close to 1.6 million tons per year (Park and Kim, 2014; Rorrer et al., 2019). This value will be annually increased since there is a massive demand for UV protection film production (Jha, 2020). However, PET is very slowly degraded by certain microorganisms (Taniguchi et al., 2019). On the other hand, the disposal of metal oxide nanoparticles is also toxic for the environment (Lee et al., 2010). Hence, developing a biodegradable film augmenting UV-light blocking is growing due to the primary concern of solving the negative environmental impacts. Since most commercial UV protection film possesses only lower than 90% of UV-light absorption (Wu et al., 2019), the production of a transparent bio-based film containing complete absorption of all UV-light transmittances will be competitive to obtain a better price.

Lignocellulosic biomasses are promising sources for biodegradable film production due to the abundant availability, renewability, and non-toxicity. They offer a key advantage over synthetic plastic films that they can be degraded by certain living organisms. Cellulose is the highest composition in lignocellulosic biomass (30-50% of biomass dry weight) (Abdel-Hamid et al., 2013). It structurally contains linear polymer chains of β-(1-4)-D-glucopyranose (Benítez and Walther, 2017). Besides cellulose, lignin in lignocellulosic biomasses also possesses interesting properties, including UV absorption (Park et al., 2019). This ability is obtained from its functional groups, such as phenolic unit, ketone, and chromophores (Huang et al., 2020). Several attempts at cellulose-lignin film development have been recently reported. Sadeghifar et al. (2017) reported that cellulose film covalently bonded with 2 wt % lignin exhibited high transparency and more than 90% UV-A protection. Wei et al. (2020) demonstrated that incorporating lignin into cellulose nanocrystal (CNC) film significantly improved its mechanical strength, UV-blocking, and antioxidant activity. Furthermore, the strong UV-light absorption, effective oxygen barrier capacity, and good antibacterial performance were successfully obtained from lignin-containing cellulose nanofiber (CNF) (Sirviö et al., 2020).

Although cellulose-lignin composite films showed promising UV-shielding properties, the certain characteristic of cellulose still has limitations. It is well known that cellulose is usually difficult to dissolve in water or some organic solvents due to its strong hydrogen bonds and a partially crystalline structure (Tian et al., 2017). Consequently, a previous attempt to directly use extracted cellulose from biomasses has been reported to possess poor film quality (Pang et al., 2013). The modification of cellulose into carboxymethyl cellulose (CMC) evidently improves its film forming properties as a water-soluble polysaccharide (Asl et al., 2017; Oun and Rhim, 2015). The attached carboxymethyl group into the cellulose chain contributes to disrupts its strong hydrogen bonds, following by further hydrogen bonding reaction with water molecule (Chua et al., 2020). Although CNC and CNF are also considered the famous water-soluble cellulose products, the presence of impurities from residual lignin could decreased their hydrophilicity that makes them not compatible with hydrophilic lignin (Herrera et al., 2018). On the other hand, further purification of CNC

and CNF needs additional cost and process. Therefore, CMC demonstrates the most desired cellulose derivative products for film preparation in this study. One of the common methods to extract both cellulose and lignin is alkaline (soda) pulping. The method was reportedly produced water-soluble lignin (Jiang et al., 2018). Thus, its hydrophilicity will be compatible with CMC to form intermolecular hydrogen bonding formation.

Empty fruit bunch (EFB) is a lignocellulosic agricultural waste in abundance from oil palm (*Elaeis guineensis* Jacq.) crop mainly grown in the tropical area of Southeast Asian countries, including Indonesia, Malaysia, and Thailand. The oil palm industry produces 1.1-1.5 tons of EFB per ton of crude palm oil (CPO) (Dahnum et al., 2015). Other oil palm residues such as mesocarp fibre and palm kernel shells are commonly burned to generate heat for boilers, especially those in local mills and electric power plants. However, EFB is not suitable for such utilization due to its high-water content; thus, it is usually left at the plantation area for composting (Ahmad et al., 2019). Due to the lack of commercial opportunities, EFB wastes in some processing mills are disposed of via open burning, contributing to dangerous air pollution and health. However, the high proportion of cellulose (34.0-40.4%) followed by lignin (23.1-29.6%) in EFB biomass can be potentially utilized to increase its economic value (Ahmad et al., 2016). Therefore, it is of interest to extract cellulose and lignin to produce a biodegradable UV protection film. An early attempt to synthesize an EFB CMC product resulted in a film with low mechanical strength (Amin et al., 2006). Hence, the process development to improve the quality of the EFB CMC film is required. The incorporation of EFB lignin will be optimized to obtain complete UV-blocking capacity.

1.2 Objective of this study

To produce biodegradable UV protection film using cellulose and lignin extracted from oil palm empty fruit bunch.

1.3 Expected beneficial outcome

Results from this study will be a basis for future commercial process development of biodegradable UV protection film production from oil palm empty fruit bunch.

1.4 Research framework

The research framework in this study is displayed in the following scheme (Figure 1).
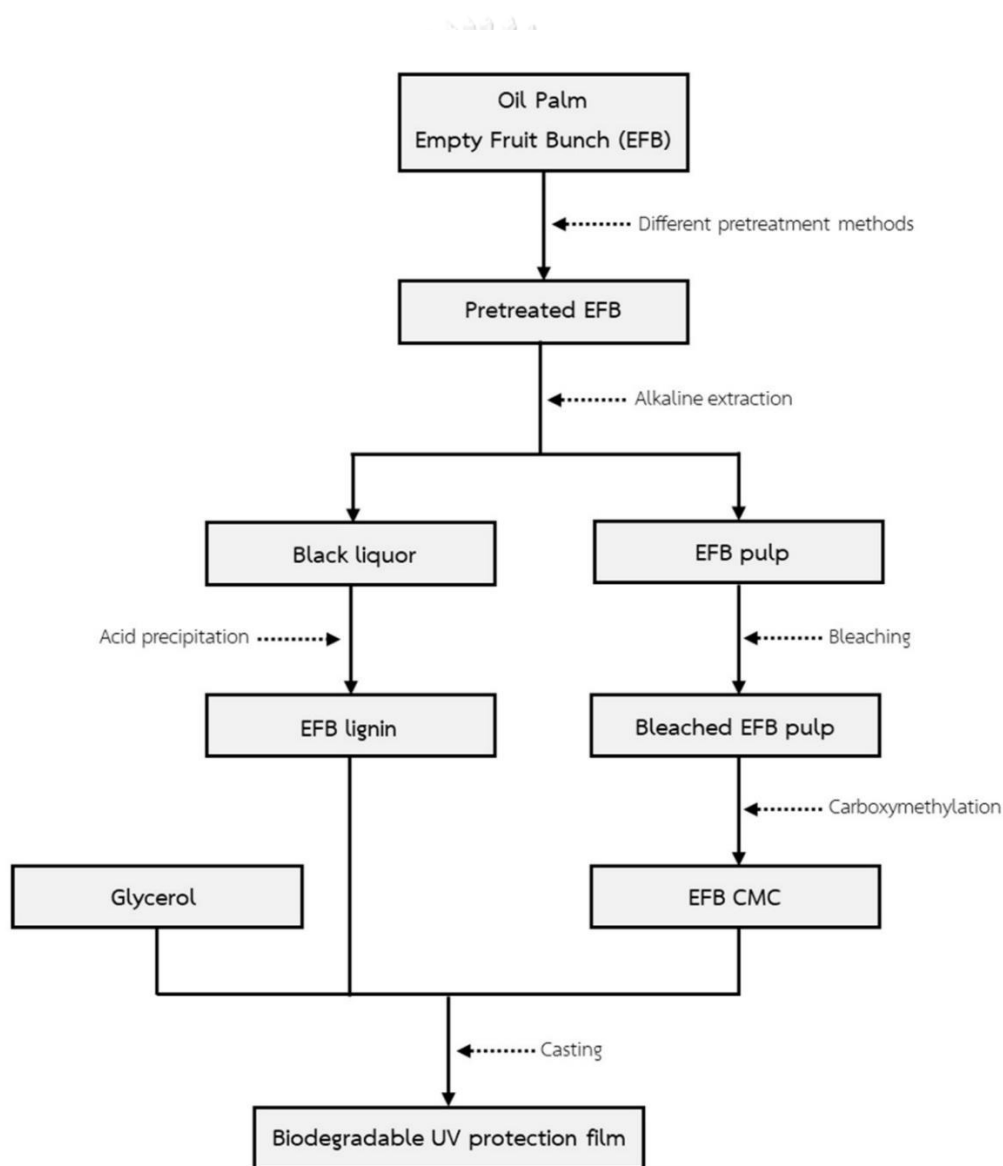
Figure 1 Research flowchart of UV protection film produced from EFB.

CHAPTER II

LITERATURE REVIEWS

2.1 UV protection film

The need to protect sensitive materials against ultraviolet (UV) light irradiation is the main objective to develop the sun-blocking product, especially utilized in outdoor applications. The UV light was characterized as UV-C (220-275 nm), UV-B (275-320 nm), and UV-A (320-380 nm) (Zhang et al., 2020). Its radiation for long periods is responsible for the photodegradation phenomenon, which strongly contributes to create some problems, such as decreasing the mechanical properties of polymers (cracking), weathering, sunburn skin, dyes discoloration, and yellowing of plastics or papers (Sadeghifar et al., 2017). Also, excessive UV light exposure can profoundly affect severe negative impacts on human health (Posoknistakul et al., 2020). Have been firstly introduced in 1970, UV blocking products were applied to overcome those problems, whereby its UV absorption capacity was determined by the sun protection factor (SPF) (Sadeghifar and Ragauskas, 2020).

A commercial polyester film product contained useful UV barrier ability when the various functional UV blocker additives were incorporated into the film matrix. The additives include some inorganic metal oxide nanoparticles such as titanium dioxide (TiO_2), zinc oxide (ZnO), silicon dioxide (SiO_2), and aluminum oxide (Al_2O_3) (Wang et al., 2019). However, those ingredients still do not bar all UV light transmittance (Zayat et al., 2007). On the other hand, their usage is also harmful to the environment when they are disposed of after utilized (Lee et al., 2010). To minimize the side effects, the significant interest to find greener innovation has been growing. A recent study has shown that biopolymer containing abundant phenolic hydroxyl groups can potentially be an alternative to be a natural UV blocker to replace those inorganic additives (Guo et al., 2019). Unlike metal oxide nanoparticles which protect materials from UV light via a reflection manner, the phenolic hydroxyl groups can block UV light via absorption of photon energy (Tian et al., 2017). A UV protection film used by consumers has a UV absorption of at least 90% (Figure 2)

(Wu et al., 2019). In this context, the capacity of a transparent film to completely block all UV light region will receive high price in the market (Sadeghifar et al., 2017).
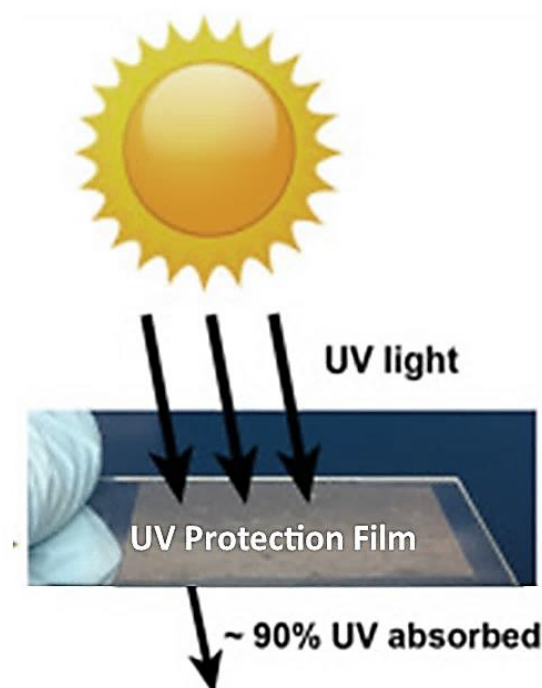
Figure 2 Illustration of UV light absorption by a UV protection film (Wu et al., 2019).

The recent application of UV protection film has been expanded largely. A commercial UV protection film product can be easily found in car windshields and clean windows. This type of film is also suitable for coating a special biological test container since some microorganisms are sensitive to UV exposure (Huang et al., 2020). Several studies also have developed the application of this film for the purpose of skin and eye protection (Almutawa et al., 2013). Contact lenses and glasses containing a UV blocking ability evidently reduced the adverse effect on the cornea and retina (Roberts, 2011). Excessive exposure to UV radiation in the wavelength of UV-A and UV-B could increase the high risk of skin cancer (Lambert et al., 2020). Several chronic effects of the skin (immunosuppression, photoaging, and photocarcinogenesis) were affected by UV exposure (Kullavanijaya and Lim, 2005). A recent study reported that UV protection film also can be applied in the active

packaging as a technology to improve the shelf-life, quality, and safety of food. The utilization of phenolic hydroxyl groups to be a natural UV blocker provides some advantages in this technology since its function is associated with food preservation as a barrier from UV light, microorganism, and free radicals (Vilela et al., 2017).

2.2 Lignocellulosic biomass

With growing concerns on the environmental issue, the use of natural resources receives extensive attention to substitute petroleum-based resources. Nowadays, Lignocellulosic biomass has been known as the most abundant renewable resource in the world with the annual production around 1.3×10^{10} metric tonnes (Hamawand et al., 2020). Therefore, it can be a prospective candidate for a sustainable biopolymer source in the future. This type of biomass comprises three major macromolecules, including cellulose, hemicellulose, and lignin. Thus, they are interwoven into a three-dimensional complex matrix (Martins et al., 2020). Sometimes, a smaller portion comprises proteins, pectin, waxes, and extractives (Naidu et al., 2018). Grass, agricultural residue, and forestry waste are examples of the most common lignocellulosic biomass easily found worldwide (Patinvoh et al., 2017). Furthermore, the proportion of their composition relates to the sources and plant species, as summarized in Table 1.

The complex structure of lignocellulosic biomass makes it difficult to be fractionated into cellulose, hemicellulose, and lignin (Figure 3). It contains a robust cellulose-hemicellulose-lignin association called biomass recalcitrant (Barakat et al., 2013). This native structure is also become the main reason for very low biodegradation by various microorganisms in nature (Brethauer and Wyman, 2010). To overcome this biomass recalcitrant, some researchers develop the pretreatment process. It was classified as thermochemical and biochemical (Laser et al., 2009). According to Kumar and Sharma (2017), the benefit of thermochemical pretreatment is a fast process and can handle a broad range of feedstock continuously, but the main drawback is its non-specific biomass deconstruction. In contrast, biochemical pretreatment is a highly selective degradation to obtain the desired product but it needs a slow process.

Table 1 Biomass composition of most common lignocellulosic materials.

Source	Biomass	Cellulose (%)	Hemicellulose (%)	Lignin (%)	References
Agriculture	Sugarcane bagasse	40.8	24.1	33.7	(Philippini et al., 2019)
	Rice husk	52.9	14.6	19.3	(Zakaria et al., 2020)
	Rice straw	28.8	55.5	11.4	(Syaftika and Matsumura, 2018)
	Corn cob	45.1	33.2	13.8	(Louis and Venkatachalam, 2020)
	Corn stover	34.3	22.9	20.9	(An et al., 2020)
	Bamboo	12.4	12.9	20.2	(Yang et al., 2021a)
	Sorghum stalk	38.7	18.8	18.7	(Zhang et al., 2019)
	Alfalfa	32.4	16.9	13.8	(Chen et al., 2020)
	Switchgrass	39.1	32.8	20.1	(Geng et al., 2018)
	Wheat straw	30.7	22.0	17.1	(Tian et al., 2018)
	Elephant grass	34.6	20.2	19.3	(Haldar and Purkait, 2020)
Forestry	Eucalyptus	37.5	28.3	39.1	(Xu et al., 2019)
	Pine	39.7	22.1	28.1	(Oh et al., 2020)
	Poplar	47.8	18.4	21.5	(Li et al., 2020b)
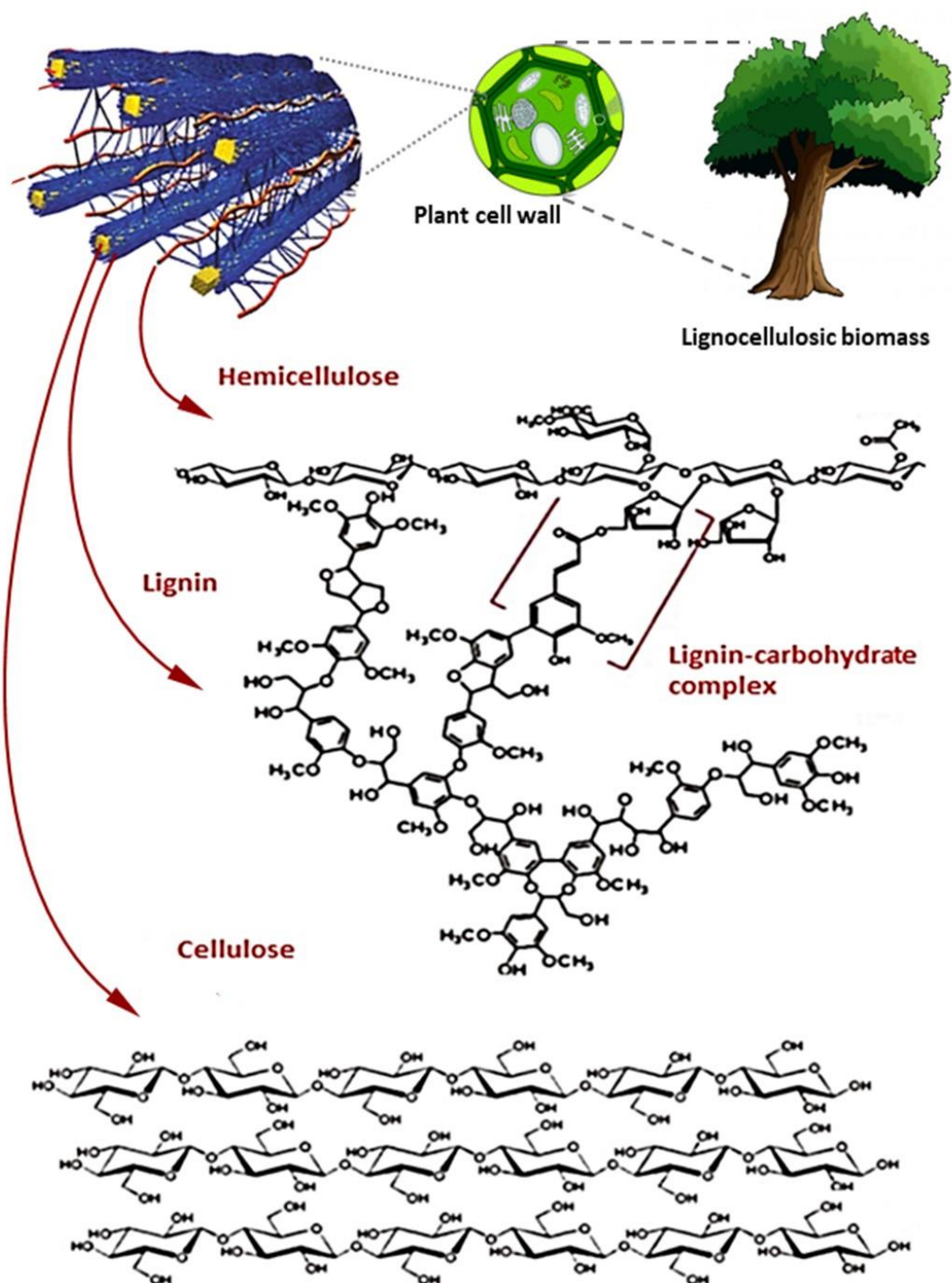
Figure 3 Lignocellulosic biomass structure (Volynets et al., 2017).

2.2.1 Cellulose

2.2.1.1 Structure and properties

Cellulose is the most abundant organic polymer on the earth (Joshi et al., 2015). Its fair yield via photosynthesis is estimated to reach 830 million metric tonnes per annum (Joshi et al., 2015). Cellulose is the major component of crops with high molecular weight (Ünlü, 2013). It is a linear polysaccharide composed of β-1,4-linked D-glucopyranose monomers (Klemm et al., 2005). In plant cell wall, cellulose provides mechanical strength and chemical stability (Yu et al., 2017). The size of cellulose molecules is conveyed according to the number of repeating anhydroglucose units on its chain, known as the degree of substitution (DP) (Trache et al., 2016). The native cellulose is non-toxic, tasteless, odorless, hydrophobic, chiral, biodegradable, and renewable, which its DP ranges from 100 to 15,000 (Klemm et al., 2005). Cellulose hydroxyl groups are partially involved in the intra- and intermolecular hydrogen bonds (Figure 4), which cause crystalline arrangements and high insoluble property (Park et al., 2010). Its crystallinity can be a major recalcitrant factor impeding its chemical and biochemical conversion (Yang et al., 2019). Production of cellulose derivatives is necessity to overcome this limitation.
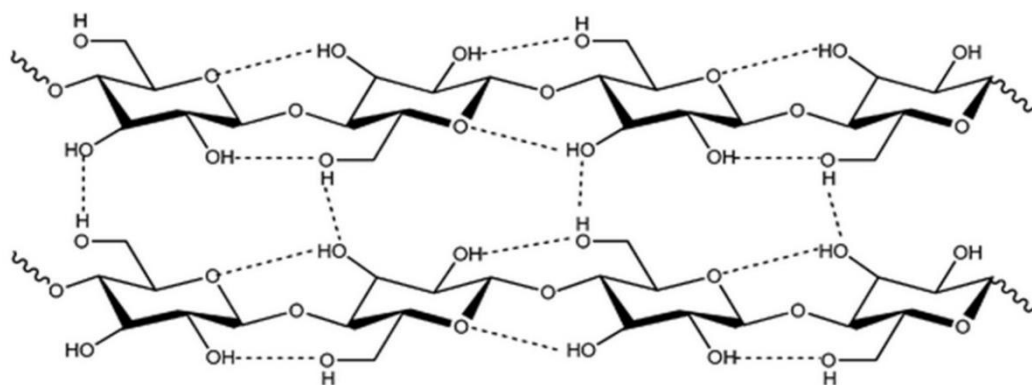
Figure 4 Cellulose crystalline structure in lignocellulosic plant (Wang et al., 2012).

2.2.1.2 Cellulose extraction process

The origin structure of cellulose in lignocellulosic plants is surrounded by a lignin-hemicellulose complex matrix (Klemm et al., 2005). Hence,

the development method for removing non-cellulosic materials is essential to produce high purity of cellulose. The most common method for this purpose is pulping process. Recently, various pulping methods are introduced and applied in the industry, such as kraft ($NaOH + Na_2S$), alkaline ($NaOH$), sulfite (Na_2SO_3), and organosolv (acetone, methanol, ethanol, butanol, ethylene glycol, formic acid, or acetic acid) (Ndaba et al., 2020). The white color of obtained pulp indicates high purity of cellulose and successful removal of other components (Dos Santos et al., 2013). Among all methods, alkaline treatment using NaOH can efficiently degrade lignin and hemicellulose following by an efficient reduction of the crystalline region in the cellulose chain, potentially giving benefits for easy cellulose modification to produce derivative products (Mittal et al., 2011).

2.2.1.3 Carboxymethyl cellulose

Carboxymethyl cellulose (CMC) is a derivative product produced from the etherification process of cellulose. In general, the synthesis consists of two-step reactions that occur in alcoholic solution (Figure 5). Firstly, cellulose was modified into alkali cellulose after reaction with sodium hydroxide (NaOH) as a catalyst, following by reaction with sodium mono chloroacetate (SMCA) to produce CMC (Joshi et al., 2015). During the process, hydroxyl groups in cellulose, mainly in C2, C3, and C6 of the glucose units, are substituted by carboxymethyl substituent ($-CH_2$-COO-) (Asl et al., 2017). Thus, it contributes to CMC's characteristics as a hydrophilic polysaccharide (Golbaghi et al., 2017). The CMC product grade depends on the degree of substitution (DS) (Barba et al., 2002). CMC is highly soluble in water when its DS value reaches < 0.4 due to its hydro affinity (Waring and Parsons, 2001). The maximum DS of CMC product is 3, indicating that all hydroxyl groups in cellulose are changed (Moussa et al., 2019). However, the DS of commercial CMC commonly ranges only from 0.4 – 1.4 (Richardson and Gorton, 2003). Nowadays, its global manufacture has been estimated to achieve 360,000 metric tonnes per year. CMC considered the most utilized cellulose ether in the world for various industrial applications such as textile, food, oil drilling, and chemicals (Candido and Gonçalves, 2016; Oun and Rhim, 2015).
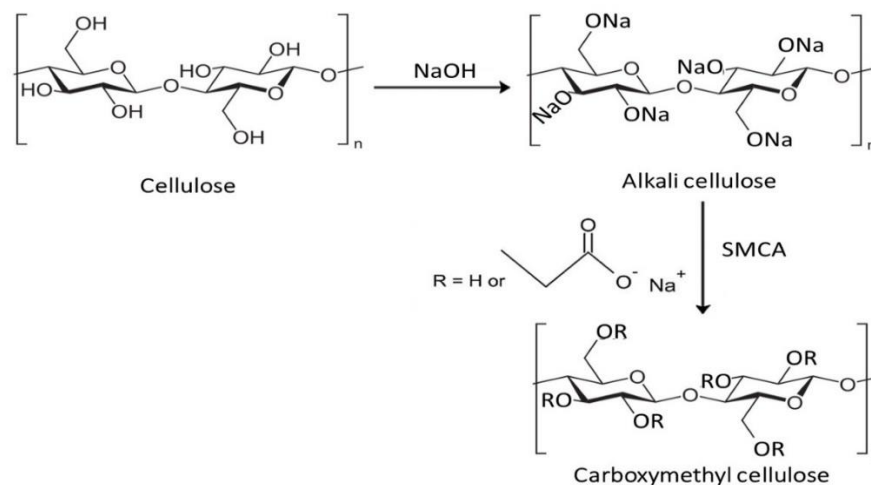
Figure 5 Two-step reaction process in carboxymethyl cellulose synthesis (Casaburi et al., 2018).

Currently, CMC has been developed to be one of the polymer matrixes in the biodegradable film production since it has great film-forming properties (Qi et al., 2016). It also offers various advantages over other biodegradable film products, such as fast biodegradability, better mechanical performance, better water vapor barrier properties, high transparency, high thermal stability, and easy to produce (de Dicastillo et al., 2016). Likewise, the CMC film is superior in oxygen, carbon dioxide, and lipid barrier capacity (Suppiah et al., 2019). CMC's non-toxic characteristic also allows it to be applied in edible film product (Lan et al., 2020). Although it showed some interesting properties, the neat CMC film does not possess the ability in UV-blocking capacity (Michelin et al., 2020). Thus, natural compounds containing phenolic hydroxyl groups should be added to improve CMC film to form a UV-protection film. However, since it has some excellent properties, CMC has been utilized to reinforce other film blends, such as gelatin-CMC film (He et al., 2020), CNC-CMC film (Li et al., 2020a), nanocellulose-CMC film (Nadeem et al., 2020), CNF-CMC film (Zabihollahi et al., 2020), starch-CMC film (Jiang et al., 2020), hemicellulose-CMC film (Weerasooriya et al., 2020), chitosan-CMC film (Wang et al., 2019), and sodium alginate-CMC film (Han et al., 2018).

2.2.1.4 Development of CMC-based film from biomass

Rachtanapun et al. (2012) developed a CMC film from cellulose isolated from durian rind. The optimum condition was found when NaOH as a catalyst at the concentration of 30% (w/v) during carboxymethylation, providing the highest viscosity and DS (0.87) of the obtained CMC product. This condition also successfully reduced the crystallinity. Further film casting revealed that CMC synthesized from the optimized condition produced the highest tensile strength (140.77 MPa) and excellent water vapor transmission rate (WVTR) (220.85 g/day.m^2). Candido and Gonçalves (2016) prepared a biodegradable CMC film from sugarcane straw. The Cellulose of the sugarcane straw was extracted by process of H_2SO_4 treatment (10% v/v) followed by NaOH extraction (5% w/v) and H_2O_2 bleaching (5% v/v). The results showed that the obtained CMC possessed a low DS (0.4) due to the availability of residual lignin, which affected poor film mechanical properties. Another study from Asl et al. (2017) reported that CMC-based film was successfully synthesized from sugarcane bagasse. Various concentrations of NaOH were tested to optimize the production of CMC with appropriate film properties. NaOH concentration at 30% (w/v) was also found to be the best composition due to its high viscosity and DS (0.78). An increase in glycerol addition (0-3%) into the CMC film significantly decreased its mechanical strength and water vapor barrier property. A biodegradable CMC film prepared from sugarcane bagasse has numerous features in the coating materials.

2.2.2 Lignin

2.2.2.1 Structure and properties

Lignin is the largest organic polymer in nature after cellulose. It composes of three primary phenolic monomers (monolignols) known as *p*-coumaryl alcohol, coniferyl alcohol and sinapyl alcohol linked together to form Cβ-O (β-O-4 aryl ether) and CC (β-5 and β-β) bonds (Hossain et al., 2019). The difference among each lignin monomer is the number of methoxy (-OCH_3) groups, as shown in Figure 6. Lignin contains a variety of functional groups, including methoxy, hydroxyl, carboxyl, and carbonyl groups. Due to these properties, it can be a potential source of

aromatic compounds and chemical products such as phenol, benzene, dimethyl sulfide, cresols, dimethyl sulfoxide, methanol, ether, and chemical mixture (Chio et al., 2019; Liu et al., 2015; Mahmood et al., 2016). The native lignin can act as an adhesive between cellulose and hemicellulose providing the rigidity to strengthen cell wall structure (Chakar and Ragauskas, 2004). Nowadays, extracted lignin is mainly used for energy purposes, while only 2% of its total production in the world is commercially utilized for value-added products (Tribot et al., 2019).
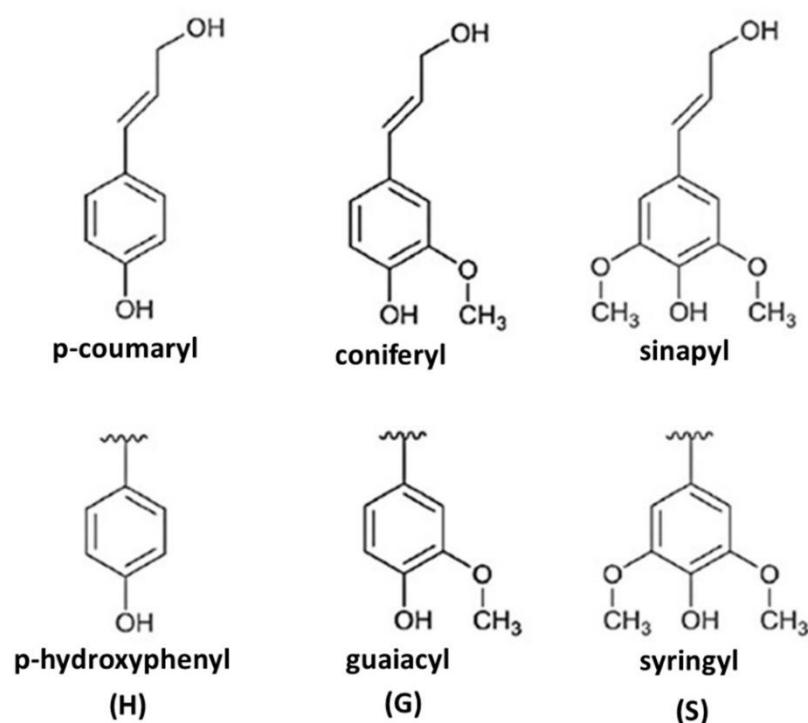
Figure 6 The precursors of lignin (Kai et al., 2016).

Lignin is the only material in the lignocellulosic plant having richness in aromatic rings due to its phenylpropanoid structure (Sadeghifar et al., 2017). These abundant phenolic units allow lignin to possess strong UV-absorption and antioxidant activity (Gerlock et al., 2001). Therefore, lignin can be used as alternative for polymer film blend to replace the usage of metal oxide in the industrial UV-blocking film fabrication. Its UV-blocking activity depends on its phenolic substructures, including hydroxyphenyl (H), guaiacyl (G), and syringyl (S).

According to Guo et al. (2019), the lignin substructure's contribution to both UV-blocking and antioxidant property from high to low was S > G > H.

2.2.2.2 Lignin extraction process

The physical and chemical structures of extracted lignin depend on plant species, growth condition, and extraction method (Kim and Um, 2020). The molecular weight of extracted lignin ranges from 1,000 to 20,000 g/mol, but its degree of substitution is difficult to calculate since lignin contains sub-units which repeat randomly (Naseem et al., 2016). The method to isolate lignin is in the same way with cellulose extraction through the pulping process. The difference is that lignin can be collected from the black liquor, a dark liquid residue resulted after pulping process, by precipitation (pH change) or ultrafiltration (Kai et al., 2016). The pulping process can cut the big polymer of lignin into the smaller chain solubilized in the black liquor (Doherty et al., 2011). Kraft and organosolv pulping have been reported to produce hydrophobic derivative of lignin whereas hydrophilic derivative of lignin can be obtained from sulfite (lignosulphonate) and alkaline pulping (Michelin et al., 2020; Zadeh et al., 2018).

2.2.2.3 Development of lignin in UV protection film application

Technical lignin does not have the ability to form film alone since the extraction process could create cleavage linkages among lignin itself, which contributes to producing small and branched lignin chains. Therefore, several attemps utilized lignin to be an additive in the film composites to improve its UV-blocking application. However, excessive concentration of lignin reportedly deteriorated film mechanical properties and reduced film transparency (Xing et al., 2017). Bian et al. (2021) reported that the high percentage of lignin in the lignocellulosic nanofibril (LCNF) film improved its UV-blocking capacity and thermal stability. Kolibaba et al. (2020) modified lignin containing anionic carboxylate groups, which enhanced chitosan-based film to possess an effective UV blockade. Besides UV protection, Yang et al. (2021b) found that lignin nanoparticles (LNP) contributed to

significant improvement on thermal stability, antioxidant, and antibacterial of PVA-based film for active food packaging.

2.3 Oil palm empty fruit bunch

Oil palm (*Elaeis guineensis* Jacq.) is one of the essential perennial crops grown in tropical regions of the world. It belongs to the family of monocotyledon (Corley and Tinker, 2003). Although oil palm is native to Africa, its plantation has been developed in many tropical countries, especially in Southeast Asia (Figure 7). Nowadays, there are five leading producing countries, including Indonesia (8,150,000 ha), Malaysia (4,620,000 ha), Thailand (720,000 ha), Nigeria (440,000 ha), and Colombia (354,000 ha) (Mba et al., 2015). Oil palm is also the most profitable global vegetable oil source accounting for more than 60% of total oilseed exports (Carter et al., 2007). Its annual oil yield is estimated to reach 58.431 million tonnes per unit cultivated area (Mba et al., 2015). The primary products of palm oil are crude palm oil (CPO) and palm kernel oil (PKO) that can be further manufactured into food, biodiesel, and oleo-chemical derivatives. CPO was extracted from the mesocarp, while PKO was obtained from the inside kernel. Currently, the edible food industry dominates their usage (90%) (Gourichon, 2019). The palm oil industry also has a side product known as palm kernel meal (PKM), commonly utilized for animal feed (Garcia-Nunez et al., 2016).
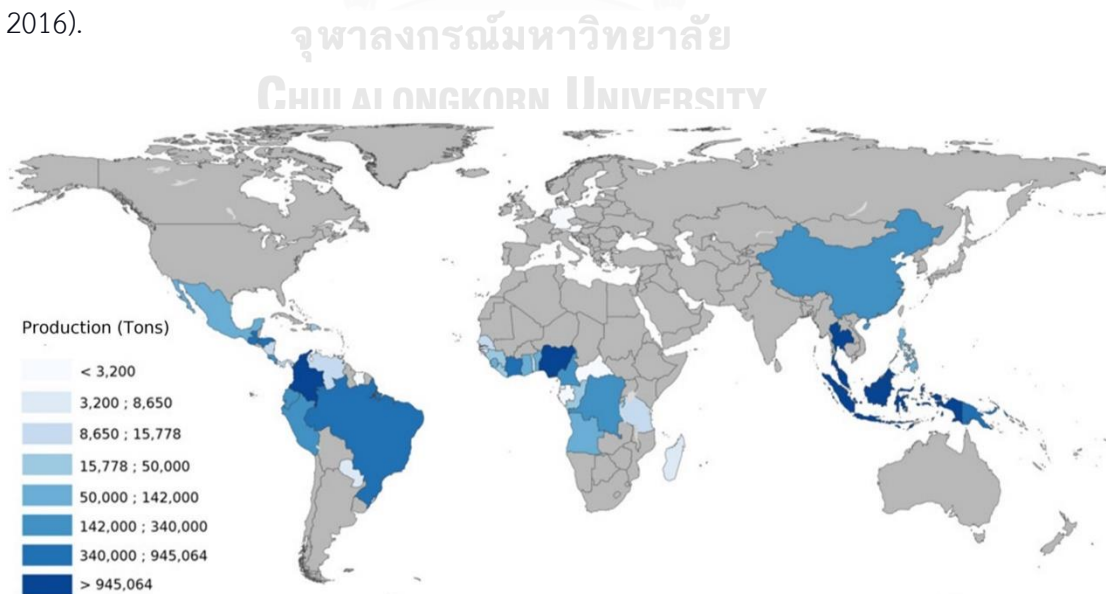
Figure 7 Distribution of oil palm plantation in the world (FAO, 2013).

An interesting fact was previously found that oil is only 10% of total dry weight in the palm, while around 90% is palm biomass (Dislich et al., 2017). Therefore, abundant lignocellulosic wastes are generated from the oil palm industry, whether from plantation or milling activities. In general, biomass residues obtained from plantation and harvesting activities are oil palm trunk (OPT) and oil palm frond (OPF) (Abnisa and Daud, 2014). OPT can be commercially used for various furniture, medium density fiber (MDF) board, and plywood (Sukiran et al., 2017). OPF is usually left in the plantation area for natural decomposition to protect soil from erosion, thus providing long-term nutrients for the crop (Rahman et al., 2014). In the meanwhile, oil palm processing mills also generate a significant source of biomass wastes, including palm kernel shell (PKS), mesocarp fiber (MF), and empty fruit bunch (EFB) (Sukiran et al., 2017). PKS and MF are commonly used to supply electricity through direct combustion (Sulaiman et al., 2010). EFB, as can be seen from Figure 8, usually contains high water content that can inhibit its ignition, contributing to the lower calorific value. Hence, EFB is unsuitable for that purpose. On the other hand, EFB wastes in some factories are often incinerated at the plant site, which harms the environment by creating dangerous white smoke pollution (Sudiyani et al., 2013).

Figure 8 Current situation of unutilized EFB wastes in some processing mills.

Although high quantity of the EFB wastes significantly contributes to negative environmental impact, its high availability will create a challenge to produce future value-added products converted from unutilized agricultural residues. EFB cellulose (23.7-65.0% of EFB dry weight) is also one of the most desired compounds that potentially can be used in the industry (Chang, 2014). Several works have reported the development of effective cellulose isolation process from oil palm EFB. Ching and Ng (2014) isolated EFB cellulose using chlorine bleaching, alkali treatment, and acid hydrolysis. The obtained EFB cellulose showed the best property at the bleaching time of 12 h, indicated by its high visible light transmittance and thermal stability. Teow et al. (2020) extracted EFB cellulose using a combination of NaOH and H_2O_2 treatment. The process effectively removed the hemicellulose and lignin substituents on the obtained EFB pulp. Furthermore, this extraction method successfully produced EFB cellulose with high crystalline phase.

The cellulose extracted from EFB to fabricate a composite film was previously reported by Zailuddin and Husseinsyah (2016). The extracted cellulose was dissolved in a mixture of N, N-Dimethylacetamide (DMAc) and lithium chloride (LiCl), following by mixing with commercial microcrystalline cellulose (CMC). The EFB cellulose with a concentration of 2% showed higher tensile strength and elastic modulus. Moreover, a much higher concentration of cellulose EFB (more than 4%) decreased all mechanical properties due to the formation of agglomerations.

The utilization of EFB cellulose for polymer blending in film production was also developed by Rahmi et al. (2017). The extracted cellulose was used to reinforce chitosan film for the application of cadmium ions removal from aqueous solutions. According to FTIR, XRD, and SEM analysis, cellulose particles displayed a significant interaction with chitosan to form a dense structure due to bonding formation. The improvement of the tensile strength value was reported after the incorporation of 10% EFB cellulose particles into the chitosan/cellulose film. In this concentration, the authors found the best composition for effective removal of Cd^{2+} from aqueous solution. Similarly, Cifriadi et al. (2017) reported the utilization of extracted EFB cellulose with high purity (97%) to improve a cassava starch blend film. The cellulose was firstly oxidized using sodium hydroxide to reduce the crystallinity and

to increase the carboxyl contents. The physical characteristic affected by glycerol loading as a plasticizer was also evaluated. The tensile strength was significantly reduced in line with the increase in the amount of glycerol concentration. In contrast, this condition had a significant contribution on improving the elongation at break value of the obtained composite film.

Amin et al. (2006) modified EFB cellulose into EFB CMC for s drug coating agent. However, the quality of EFB CMC is quite lower than a commercial CMC. EFB CMC film exhibited 7.85-14.79 MPa of tensile strength, while the commercial CMC film possessed 21.72-35.14 at a similar concentration. Furthermore, SEM analysis indicated a rougher surface of EFB CMC film contributing to lower transparency than the commercial CMC film product.

Besides cellulose, several authors have improved the lignin extraction method from EFB. Sidik et al. (2013) collected EFB lignin using the liquefaction method with 1-butyl-3-methylimidazolium chloride ([BMIM]Cl) ionic liquid (IL) in the presence of H_2SO_4 as a catalyst. The obtained EFB lignin demonstrated its good performance with a yield of 26.6%. Tang et al. (2020) treated EFB with aqueous NaOH and aqueous NH_3 solutions. A low temperature-long time replenished treatment (LTLt-Rep-NH_3) revealed the optimized condition, producing recovered lignin at 33%. However, the potential of lignin isolated from EFB waste to be a film additive is still not explored widely. There is only one literature provided by Bhat et al. (2013) that they utilized the lignin for reinforcement of sago (*Metroxylon sago*) starch-based film for food packaging application. They found that addition of lignin significantly improved the thermo-mechanical properties, seal strength, and water resistance. Furthermore, lignin successfully reduced vapor permeability of the composite film indicating its superior performance in barrier of water vapor molecule.

CHAPTER III

MATERIALS AND METHODS

3.1 Materials and Equipment

- Autoclave: Model 7SX, Foundry Co., Inc, USA

- Autopipette: Dragon-Lab, China

- Centrifuge: Hettich, Germany

- Contact angle goniometer: Model DM100, Kyowa Interface Co., Ltd, Japan

- Fourier infrared spectrophotometer: Model 6700, Thermo Nicolet Corp, USA

- Hot air oven: Model B30, Memmert, Germany

- Hot plate magnetic stirrer: C-MAG HS10, Sigma Aldrich, USA

- Micrometre screw gauge: Mitutoyo, Japan

- Particle size analyser: Model Mastersizer 2000, Malvern Instrument Ltd, UK

- pH meter: Model PP-50, Sartorius, Germany

- Quick cold coater: Model SC-701MC, Sanyu Denshi Co., Ltd, Japan

- Reflectance spectrophotometer: Macbeth, USA

- Rheometer: Model Physica MCR 301, Anton Paar, Germany

- Scanning electron microscope: Model TM3030 Plus, Hitachi, Japan

- Spectrophotometer: Model V-570, Jasco Corp., Japan

- Thermogravimetric analyser: Model Q50, TA Instruments, Inc., USA

- Universal testing machine: LTS-500N-S2, Minebea Co., Ltd, Japan

- Vortex: Charan Associates Co., Ltd, Thailand

- Weight balance, 2 digits: Model BL610, Sartorius, Germany

- Weight balance, 4 digits: Model AB204-S/FACT, Mettler Toledo, USA

3.2 Chemicals

- Acetic acid: Ajax Finechem, New Zealand

- Acetone: Thananan Chemical Co., Ltd, Thailand

- Carboxymethyl cellulose: Sigma Aldrich, USA

- Cellulose: Sigma Aldrich, USA

- Cetyl trimethylammonium bromide (CTAB): Ajax Finechem, New Zealand

- Disodium ethylenediamine tetraacetate (EDTA) dehydrate: Ajax Finechem, New Zealand

- 95% ethanol: Thananan Chemical Co., Ltd, Thailand

- Ethylene glycol monoethyl ether: Ajax Finechem, New Zealand

- Hydrochloric acid: Carlo Erba, Italy

- Hydrogen peroxide: Chem-supply Pty Ltd, Australia

- Iron (III) nitrate nonahydrate: Ajax Finechem, New Zealand

- Isopropanol: Fisher Scientific, UK

- Methanol: Merck, Germany

- Nitric acid: QRêc, New Zealand

- Oxalic acid: Ajax Finechem, New Zealand

- Potassium acetate: Ajax Finechem, New Zealand

- Potassium Bromide: Fisher Scientific, UK

- Potassium Permanganate: Sigma Aldrich, USA

- Silver nitrate: Carlo Erba, Italy

- Silver sulphate: Carlo Erba, Italy

- Sodium borate decahydrate: Ajax Finechem, New Zealand

- Sodium hydrogen phosphate: Merck, Germany

- Sodium hydroxide: Ajex Finechem, New Zealand

- Sodium lauryl sulphate: Ajax Finechem, New Zealand

- Sodium monochloroacetic acid: Merck, Germany

- Sulfuric acid: QRêc, New Zealand

- Tertiary butyl alcohol: Ajax Finechem, New Zealand

3.3 Procedures

3.3.1 Screening for suitable pretreatment

EFB collected from an oil palm mill industry, PT. Tritunggal Sentra Buana, was firstly cut to small pieces, ground, and sieved to fine powder (≤ 1 mm) followed by drying at 60°C in a hot air oven until it reached a constant weight. Three types of chemical pretreatments, including hot water, alkaline (6% (w/v) NaOH), and acid (0.5% (v/v) H_2SO_4), were performed according to Vena et al. (2013). Each

pretreatment was carried out in an autoclave (121°C, 15 lbs per square inch) for 40 mins with a solid/liquid ratio of 1:6. The pretreated EFB was then neutralized with a large volume of distilled water, followed by oven drying at 60°C.

3.3.2 Extraction

Alkaline extraction was employed to isolate cellulose from each pretreated EFB. The sample (100 g) was mixed with 15 g NaOH (to the final concentration of 15% (w/v)), and distilled water (1000 mL) was then added at a solid/liquid ratio of 1:10. The mixture was incubated in an autoclave (121°C, 15 lbs per square inch) for one h. The EFB pulp was separated from black liquor by filtering through a fabric sieve. The black liquor was kept in an opaque bottle at room temperature for further lignin precipitation. The obtained pulp was then washed with distilled water until it reached neutral pH and oven dried at 60°C.

3.3.3 Bleaching

Totally chlorine-free bleaching was conducted to increase the cellulose purity according to the protocol introduced by Tristantini and Yunan (2018). Briefly, five grams of EFB pulp was added into 100 mL of 10% (w/v) H_2O_2 solution at 80°C for two h under continuous stirring conditions. After that, the bleached pulp was filtered, washed with distilled water to reach neutral pH, and oven dried at 60°C.

3.3.4 Lignin precipitation

The EFB lignin precipitation was performed by gradually adding glacial acetic acid to the black liquor until pH 7 was reached. The precipitated lignin was harvested by centrifugation (Universal 320R, Tuttlingen, Germany) at 12,000 x g (6,000 rpm) for 10 mins and oven dried overnight at 60°C.

3.3.5 CMC synthesis

CMC was synthesized from the EFB cellulose based on the procedure from Asl et al. (2017) with slight modifications. Briefly, five grams of the EFB pulp was weighed and treated with 20 mL of 30% (w/v) NaOH in 200 mL of isopropanol at room temperature for 30 min to produce alkali cellulose. After that, the suspension

was mixed with five g sodium mono chloroacetate (SMCA) and continually stirred at 60°C for 4 h. The liquid was then poured out and discarded, and the solid fraction was dispersed in absolute methanol (150 mL). The mixture was then neutralized with glacial acetic acid and filtered through a plastic sieve. The solid CMC was washed with a large volume of 70% ethanol to remove unwanted by-products. The obtained EFB CMC was rewashed with absolute methanol and oven dried at 60°C. For comparison, a commercial **α**-cellulose (C8002, Sigma-Aldrich) was also modified into CMC following the same procedure.

3.3.6 EFB CMC film production

EFB CMC films were prepared by using a casting method. Film solution containing EFB CMC (2.5% (w/v)) and glycerol (0.5% (w/v)) was stirred at 60°C and then poured into a polyacrylic film mould and oven dried at 60°C for 24 hours. EFB lignin was added into the EFB CMC solution to the final concentrations ranging from 0% to 0.3% (w/v). All dried films were carefully peeled off the mould and kept inside a desiccator containing silica gel at least 24 h before further assessments. The films prepared from commercial CMC (C5678, Sigma-Aldrich) and **α**-cellulose CMC were used for properly comparisons.

3.3.7 Characterization of biomass, CMC, lignin, and film
3.3.7.1 Determination of biomass composition

The biomass compositions of EFB and the obtained pulp, including cellulose, hemicellulose, and lignin, were determined according to Goering and Van Soest (1970).

3.3.7.2 Water solubility

The water solubility test of EFB CMC was performed according to Shui et al. (2017) with a slight modification. One gram of EFB CMC powder was dissolved in 100 mL distilled water and continuously stirred at 60°C for 1 h. The solid residue was then weighed after collected by centrifugation (Universal 320R, Tuttlingen, Germany) at 12,000 x g (6,000 rpm) for 10 min and oven dried at 60°C.

The water solubility was calculated as the percentage of dissolved EFB CMC to the total EFB CMC tested.

3.3.7.3 Degree of substitution

The degree of substitution (DS) of the CMC was measured by potentiometric titration (Haleem et al., 2014). One gram of the CMC and 50 mL 95% ethanol were mixed under stirring conditions. Then, five mL of 2 M nitric acid was added to the mixture with continuous stirring for 10 min. Next, the mixture was heated for 5 min using a hot plate following by further stirring for 20 min. The liquid was removed through filtration using filter paper (Whatman no. 1), and the precipitated CMC was washed with 100 mL 95% ethanol following by oven drying at 60°C. The obtained CMC (0.5 g) was mixed with 100 mL distilled water and 25 mL 0.5 M NaOH under continuous stirring. Then, the mixture was heated for 20 min and cooled down to room temperature. A few drops of phenolphthalein as an indicator were added to observe the color change during titration with 0.3 M HCl. The DS of CMC was calculated by using the following equation (Haleem et al., 2014):

$$A = \frac{(BC - DE)}{F} \tag{1}$$

$$DS = \frac{(0.162 \times A)}{(1 - 0.0058 \times A)} \tag{2}$$

where A was required acid per gram of CMC (mL), B was the volume of used NaOH (mL), C was the NaOH concentration (%), D was required HCl (mL), E was HCl concentration (%), F was the weight of CMC (g), 162 was the anhydrous glucose molecular weight, and 58 was the increase of net molecular weight in anhydrous glucose after each substitution of carboxymethyl group.

3.3.7.4 Viscosity

The viscosity of CMC was determined using a rheometer (Physica MCR 301, Anton Paar, Germany). The prepared CMC powder was dissolved in distilled water (2.5% (w/v)) and measured under ambient conditions with a shear rate of 100 s^{-1} (Shui et al., 2017).

3.3.7.5 Lignin particle size

The particle size of the extracted EFB lignin was measured using a laser-based particle size analyser (Mastersizer 2000, Malvern Instrument Ltd., U.K.).

3.3.7.6 Lignin purity

The purity of the extracted EFB lignin was determined using a klason lignin protocol (Itoh et al., 2003). Lignin powder (0.3 g) was added into 4.5 mL 72% (v/v) H_2SO_4 solution with continuous stirring for 2 h. Then, the mixture was filtered through filter paper (Whatman no. 1), washed, and dried at 105°C until it reached a constant weight. The lignin purity was calculated as the percentage of final weight to initial weight of EFB lignin tested.

3.3.7.7 Fourier Transform Infrared (FTIR) spectroscopy

Infrared spectra of the samples were recorded in the wavenumber between 4000 and 500 cm^{-1} using the FTIR spectrometer (Nicolet 6700, Thermo Nicolet Corp, Madison, USA). Before testing, each sample was mixed with potassium bromide (KBr) at a ratio of 1:10 and pelletized together.

3.3.7.8 Scanning electron microscopy

The samples were firstly gold coated using a quick cold coater (SC-701MC, Sanyu Denshi Co., Ltd., Japan) before analysis. The surface morphology was observed using a scanning electron microscope (SEM) (TM3030 Plus, Hitachi, Japan) at an accelerating voltage of 15 kV and magnifications of 500x for EFB biomass and 1,500x for films.

3.3.7.9 Color measurement

A reflectance spectrophotometer (Color-eye 7000, Macbeth, New York, USA) was used to determine the color of film samples and recorded some parameters, including *L* (lightness-brightness), *a* (redness-greenness), and *b* (yellowness-blueness). Furthermore, the total color difference (Δ*E*) was calculated based on the equations described by Jouki et al. (2013).

$$\Delta E = \sqrt{(L^*-L)^2 + (a^*-a)^2 + (b^*-b)^2}$$ (3)

where L^*, a^* and b^* were the standard value, and L, a and b were the film sample values.

3.3.7.10 Thickness

A micrometre screw gauge (Mitutoyo, Japan) with a minimum division of 0.01 mm was used to randomly measure the average thickness of the prepared films at ten different areas.

3.3.7.11 Water contact angle

A sessile drop method using a contact angle goniometer (DM100, Kyowa Interface Science Co., Ltd., Japan) was performed to measure the water contact angle of the film samples. Distilled water was injected by a micro syringe on the horizontal surface of prepared films (2×2 cm^2).

3.3.7.12 Water vapor permeability

The water vapor permeability (WVP) was examined gravimetrically using a cup method following the ASTM E96 (Cazón et al., 2019). Firstly, 15 mL of distilled water was transferred to the cup (5 cm in diameter and 4 cm depth). The film was then cut in a circular shape and sealed with silicone adessive on the top of the cup. After that, the cup was placed in a box containing silica gel. The WVP tests were carried out at 30°C by measuring the water weight every hour for at least eight h until the slope of the linear regression of weight loss versus time ($r^2 = 0.99$) was obtained. The WVP (g m^{-1} s^{-1} Pa^{-1}) was calculated according to the following equation (Cazón et al., 2019):

$$WVP = \frac{\Delta w \cdot x}{\Delta t \cdot A \cdot \Delta P}$$ (4)

where Δw was the loss weight of the cup (g), x was the average thickness of the film (m), Δt was the time unit (s), A was the exposed area (m^2), and ΔP (4245 Pa) was the difference in partial water vapor pressure across the two sides of the film at 30°C.

3.3.7.13 Thermogravimetric analysis

The thermal stability of the CMCs, the EFB lignin, and the prepared films was determined by thermogravimetric analyser (TGA Q50, TA Instrument, Inc., DE) from $30^{\circ}C$ to $600^{\circ}C$ at a rate of $10^{\circ}C$ min^{-1}. Each sample (five mg) was analysed at a flow rate of 20 mL min^{-1} under a nitrogen atmosphere.

3.3.7.14 Antioxidant activities

The antioxidant activity of the films was measured using the DPPH (2, 2-diphenyl-1-picrylhydrazyl) free radical scavenging assay based on the procedure of Shankar et al. (2019) with slight modifications. Each film (250 mg) was firstly dissolved in 5 mL distilled water. Then, the aqueous solution of the film (100 µL) was mixed with 900 µL of 0.1 mM DPPH methanolic solution. The mixture was then incubated for 30 min in the dark at room temperature ($20\pm5^{\circ}C$). The absorbance was measured at 518 nm (Spectrophotometer V-570, Jasco Corp., Japan) and the antioxidant activity was calculated according to the following equation (Shankar et al., 2019):

$$\text{Antioxidant activities (\%)} = \frac{A - B}{A} \times 100 \qquad (5)$$

where A was the absorbance of DPPH and B was the absorbance of DPPH containing film solution. The half-maximal inhibitory concentration (IC_{50}) was obtained after measuring antioxidant activity of the film solution at least five concentrations ranging from 0.25 – 4 mg mL^{-1}.

3.3.7.15 UV-vis spectrophotometry

The UV protection capacity of the films (2 x 1 cm^2) was evaluated by a UV-vis spectrophotometer (V-570, Jasco Corp., Japan) at the wavelengths between 275 and 320 nm and between 320 and 380 nm for UV-B and UV-A, respectively (Zhang et al., 2020). The percent transmittance at the wavelength of 550 nm was used to determine the film transparency.

3.3.7.16 Mechanical properties

The mechanical properties of the films including tensile strength, elongation at break, and Young's modulus were determined using a universal testing machine (LTS-500N-S2, Minebea Co., Ltd., Japan) equipped with a load cell of 500 N (ASTM D882). The prepared films (10 x 1 cm^2) were stretched at a rate of 10 mm min^{-1} after inserted between two jaws of the machine (5 cm gauge length).

3.3.7.17 Biodegradability analysis

The biodegradation capacity of the films was carried out by a composting test in the soil following the procedure from Riaz et al. (2020) with a slight modification. The soil used in this experiment was collected from a garden at Department of Botany, Chulalongkorn University. It was placed in a small plastic tray (8 cm in diameter and 5 cm depth). The films (2 x 2 cm^2) were then buried (2 cm depth) at ambient temperature and were dug out every week to observe the change in appearance until they were completely degraded. The soil was sprayed with 5 mL distilled water in the morning and evening.

3.3.8 Statistical analysis

All data were presented as average value ± one standard deviation derived from three replications and statistically analysed using IBM SPSS Statistics 22 (IBM Corp., Armonk, NY, USA). The one-way analysis of variance (ANOVA) followed by Duncan's multiple range test (DMRT) was applied to compare any significant differences among average values at the level of $p < 0.05$.

CHAPTER IV
RESULTS AND DISCUSSION

4.1 Screening for efficient EFB cellulose preparation

4.1.1 Cellulose extraction

Oil palm EFB used as the raw material in this study consisted of 43.17% cellulose, 23.24% hemicellulose, 14.97% lignin, and 0.97% ash (Table 2). Other contents (17.65%) found in EFB was probably extractives. This value was comparable with total extractive content found in Malaysian EFB (15%) previously reported by Nurul Hazirah et al. (2014). Generally, the EFB compositions in this study were in line with those previous study reported by Chang (2014), who described that cellulose, hemicellulose, and lignin contents found in EFB were commonly accounted for 24-65%, 21-34%, 14-31%, respectively. To extract cellulose from EFB, a chemical pulping process using 15% NaOH (w/w), commonly called alkaline extraction, was employed since it was reportedly effective for breaking down β-O-4 aryl ether bonds in lignin, leading to disintegration of its polymeric structure and cellulose release (Santos et al., 2013). After alkaline extraction, the cellulose content in the EFB pulp was significantly increased up to 0.5-fold (65.43%). Nevertheless, the residual lignin (12.42%) and hemicellulose (16.74%) were still high (Table 3) since lignin and hemicellulose are linked via a complex structure (Volynets et al., 2017), that was likely resistant to NaOH.

Table 2 Biomass composition of oil palm EFB.

No	Composition	Quantity (g/100 g EFB)
1	Cellulose	43.17 ± 1.11
2	Hemicellulose	23.24 ± 0.95
3	Lignin	14.97 ± 1.37
4	Ash	0.97 ± 0.58
5	Others*	17.65 ± 1.33

*Possibly extractives.

Table 3 Effect of different pretreatment methods and bleaching on composition of EFB pulp obtained by alkaline extraction.

No	Condition		Pulp yield	Composition (%)		
	Pretreatment	Bleaching	(g/100g EFB)	Cellulose	Hemicellulose	Lignin
1	Untreated	-	62.03 ± 0.52^a	65.43 ± 0.33^e	16.74 ± 0.95^a	12.42 ± 1.08^a
2	Untreated	✓	53.24 ± 0.27^c	67.45 ± 1.57^d	14.96 ± 0.95^b	11.56 ± 0.68^{ab}
3	Hot water	-	56.89 ± 0.73^b	71.84 ± 0.84^c	14.44 ± 0.87^b	8.84 ± 1.30^c
4	Hot water	✓	51.21 ± 0.36^d	72.14 ± 0.88^c	13.73 ± 0.41^b	8.63 ± 0.19^c
5	Alkaline	-	50.56 ± 0.46^d	74.98 ± 1.58^b	10.48 ± 1.03^c	8.60 ± 0.90^c
6	Alkaline	✓	44.78 ± 0.45^e	75.96 ± 0.83^b	8.14 ± 0.60^d	7.85 ± 0.86^c
7	Acid	-	38.33 ± 0.86^f	82.26 ± 0.72^a	2.17 ± 0.48^e	10.69 ± 0.57^b
9	Acid	✓	35.01 ± 0.57^g	83.42 ± 0.88^a	2.00 ± 0.43^e	8.79 ± 0.21^c

Different superscript letters in the same column indicated significant different values at $p < 0.05$.

To increase the EFB cellulose yield and purity for subsequent CMC synthesis, pretreatment and bleaching steps were employed to enhance the effective separation of cellulose from the surrounding hemicellulose and lignin. All three pretreatments chosen in this study were common protocols used in commercial and experimental pulping process (Vena et al., 2013). A totally chlorine-free bleaching using H_2O_2 was selected since it was environmentally friendly alternatives to the conventional chlorine bleaching which generates hazardous chlorinated organic pollutants (Fernández-Rodríguez et al., 2017). As expected, the application of various pretreatment methods prior to alkaline extraction contributed to the significant increase of cellulose content compared to unpretreated EFB, yielding 71.84%, 74.98%, and 82.26% for hot water, NaOH, and H_2SO_4 pretreatment, respectively. This was similar to the report by Akhtar et al. (2015) that H_2SO_4 pretreatment prior to NaOH extraction could significantly improve cellulose composition in EFB pulp. On the other hand, the residual lignin was also reduced significantly at 8.84%, 8.60%, and 10.69% for hot water, NaOH, and H_2SO_4 pretreatment, respectively. It has also been reported that the best lignin removal was observed when the *Eucalyptus* biomass was pretreated by NaOH, following by hot water and H_2SO_4 (Saito et al., 2016). After H_2O_2 bleaching process, a significant reduction (3-9%) in pulp yield was observed in every extraction. Although the bleaching step did not significantly increase the cellulose content, it slightly enhanced the removal of hemicellulose and lignin from the extracted pulp (Table 3).

Considering that the highest cellulose content following by the lowest hemicellulose and lignin was the goal of EFB extraction, the extraction protocol consisting of H_2SO_4 pretreatment-alkaline extraction-H_2O_2 bleaching gave the best result with 83.42% cellulose, 2.00% hemicellulose, and 8.79% lignin. The H_2SO_4 pretreatment was able to cleave the glycosidic bonds between lignin and hemicellulose effectively (Liu et al., 2018). Therefore, the remaining hemicellulose content in the EFB pulp was decreased to the lowest value in this study (2.00%). The significant reduction of hemicellulose was desired in this study since it was unwanted materials in film fabrication. Huang et al. (2019) suggested that the better removal of hemicellulose is one of the key factors for obtaining high cellulose content pulp. The

optimized extraction protocol in this study yielded a higher cellulose content (83.42%) compared to the previously reported EFB cellulose (76.45%) prepared by 0.7% sodium chlorite (NaClO$_2$) bleaching process followed by alkaline extraction using 17.5% NaOH (Parid et al., 2018).

4.1.2 CMC production

The EFB pulps (Figure 9) obtained from various extraction protocols were further carboxymethylated through a two-step reaction. Theoretically, the OH groups of the EFB cellulose were firstly reacted with NaOH which replaced protons with sodium ions. The second step was etherification with SMCA to form carboxymethyl groups (Bhandari et al., 2012). Therefore, the highest CMC yield was expected from the EFB pulp obtained from the optimized extraction protocol since it contained the highest cellulose and the lowest hemicellulose and lignin contents. Surprisingly, the highest yield of carboxymethylated product was obtained from the unpretreated-unbleached EFB pulp despite the lowest cellulose and highest hemicellulose and lignin contents (Table 4). This was likely due to the carboxymethylation of lignin rather than hemicellulose. When total sugar contents in the EFB pulps, glucose from cellulose and heterosaccharides from hemicellulose, were considered, the lowest number was found in the unpretreated-unbleached pulp (Table 4). Therefore, cellulose and hemicellulose could not be the contributing factor to the high yield of this CM product. Moreover, even though the OH groups of hemicellulose could be substituted, their availability should be low due to the majority of pentose sugars, branching structure and acetyl substitution (Tarasov et al., 2018). It has been reported that lignin can be carboxymethylated through the same reaction as cellulose (Gan et al., 2013; Kazzaz et al., 2019; Konduri et al., 2015). It also yields unwanted by-products such as glycolic and sodium glycolate that contributed the product weight increase (Kazzaz et al., 2019; Shui et al., 2017). The carboxymethylation of lignin could compete with that of cellulose and might result in low degree substitution and low water solubility of the CMC. The carboxymethylated product obtained from the unpretreated-unbleached pulp had the significantly lowest water solubility (45.51%) whereas the EFB CMC derived from

EFB pulp prepared by H_2SO_4 pretreatment-NaOH extraction-H_2O_2 bleaching exhibited the highest water solubility (81.32%) (Table 4). Therefore, despite its lowest yield the CMC obtained from this optimized extraction protocol was considered the most suitable for the subsequent film preparation.
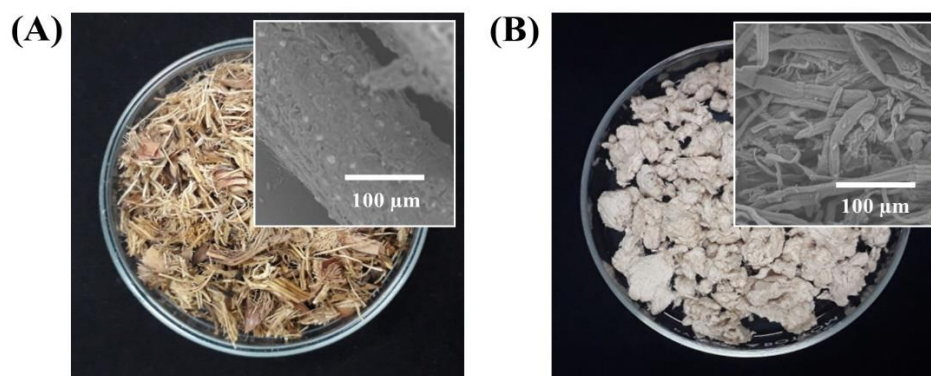
Figure 9 Morphological appearance of the untreated EFB (A) and the treated EFB pulp (B) via photographic image and scanning electron microscopy (inset).

4.1.3 Characterization of selected synthesized EFB CMC
4.1.3.1 Degree of substitution

The measurement of degree of substitution (DS) was performed to assess the quality of the synthesized EFB CMC compared to the commercial CMC and the α-cellulose CMC (Table 5). The DS indicated the amount of -OH groups in cellulose successfully substituted by carboxymethyl groups. The EFB CMC possessed a higher average DS value (1.30) than that of the commercial CMC (1.13). Due to its high purity, α-cellulose CMC achieved the highest average DS value (1.45). In this study, the EFB CMC contained 8.79% residual lignin causing a light brownish color, while both commercial CMC and α-cellulose CMC, without lignin contamination, were white in color (Figure 10). The DS value of the synthesized EFB CMC in this study was higher than those prepared from other biomasses, such as rice stubble (0.64) (Rodsamran and Sothornvit, 2017), seaweed (0.51) (Lakshmi et al., 2017), sugarcane bagasse (0.78) (Asl et al., 2017), and cotton gin (0.87) (Haleem et al., 2014).

Table 4 Effect of different pretreatment methods and bleaching to obtain EFB pulp on the yield and water solubility of CMC product.

No	Condition		Total sugars	CMC yield	Water solubility
	Pretreatment	Bleaching	(%)	(g/100 g EFB pulp)	(%)
1	Untreated	-	82.17 ± 0.69^d	147.52 ± 2.44^a	45.51 ± 0.48^{de}
2	Untreated	✓	82.41 ± 1.10^d	146.70 ± 4.81^a	48.63 ± 4.19^{cde}
3	Hot water	-	86.29 ± 1.16^a	139.44 ± 1.01^b	43.62 ± 4.57^{de}
4	Hot water	✓	85.87 ± 0.56^{ab}	146.53 ± 1.10^a	54.65 ± 3.52^c
5	Alkaline	-	85.46 ± 0.10^{abc}	127.31 ± 0.77^c	42.37 ± 0.03^e
6	Alkaline	✓	84.10 ± 0.28^c	127.32 ± 1.03^c	49.69 ± 4.53^{cd}
7	Acid	-	84.43 ± 0.61^{bc}	108.28 ± 0.96^e	65.61 ± 2.04^b
8	Acid	✓	85.42 ± 0.95^{abc}	114.19 ± 1.95^d	81.32 ± 1.53^a

Different superscript letters in the same column indicated significant different values at $p < 0.05$.

4.1.3.2 Viscosity

The viscosity of the synthesized CMC products was determined at 2.5% (w/v) with a shear rate of 100 s^{-1}. It could be seen that the α-cellulose CMC had the highest viscosity (41.81 mPa s), followed by the EFB CMC and the commercial CMC (19.92 and 18.54 mPa s, respectively) (Table 5). These results had the same trend as their DS. It seemed that the high DS value affected the increased viscosity. A previous study from Shui et al. (2017) also demonstrated that increasing DS of CMC products could improve its water solubility and viscosity. The increasing DS value provided more hydrophilic groups; thus, it enhanced the ability of CMC to form intermolecular bonding formation with water molecules (Asl et al., 2017).

Table 5 Degree of substitution and viscosity of various CMC products used for film preparation.

No	Sample	DS	Viscosity (mPa s)
1	Commercial CMC	1.13 ± 0.03^{c}	18.54 ± 0.86^{b}
2	α-cellulose CMC	1.45 ± 0.06^{a}	41.81 ± 1.44^{a}
3	EFB CMC	1.30 ± 0.01^{b}	19.92 ± 1.66^{b}

Different superscript letters in the same column indicated significant different values at $p < 0.05$.
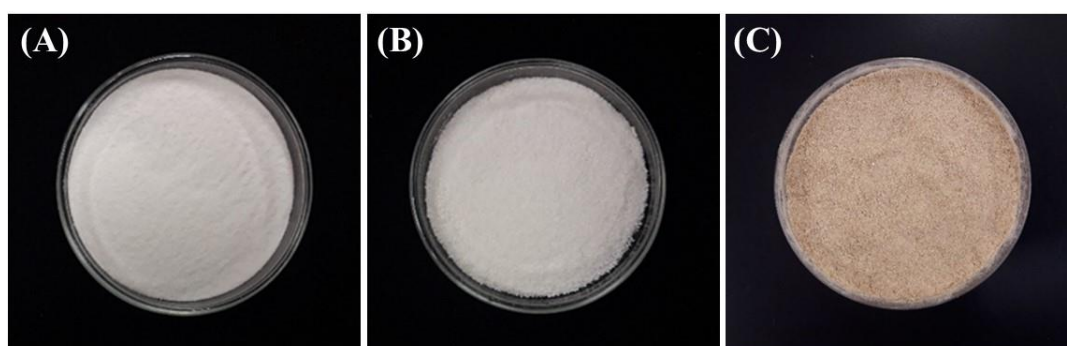
Figure 10 Visual appearance of various CMC products used for film preparation: Commercial CMC (A), α-cellulose CMC (B), and EFB CMC (C).

4.1.3.3 FTIR spectra

The structural analysis of all CMC products was determined using FTIR spectroscopy at spectra ranging from 4000 to 500 cm^{-1}. As shown in Figure 11, a broad absorption peak observed at 3402 cm^{-1} could be assigned to the stretching vibration of a hydroxyl group (-OH) (Jiang et al., 2017). After etherification, the peaks found at 1604 and 1419 cm^{-1} was due to the successful carboxymethyl substitution in the EFB CMC and α-cellulose CMC (Rachtanapun et al., 2012).
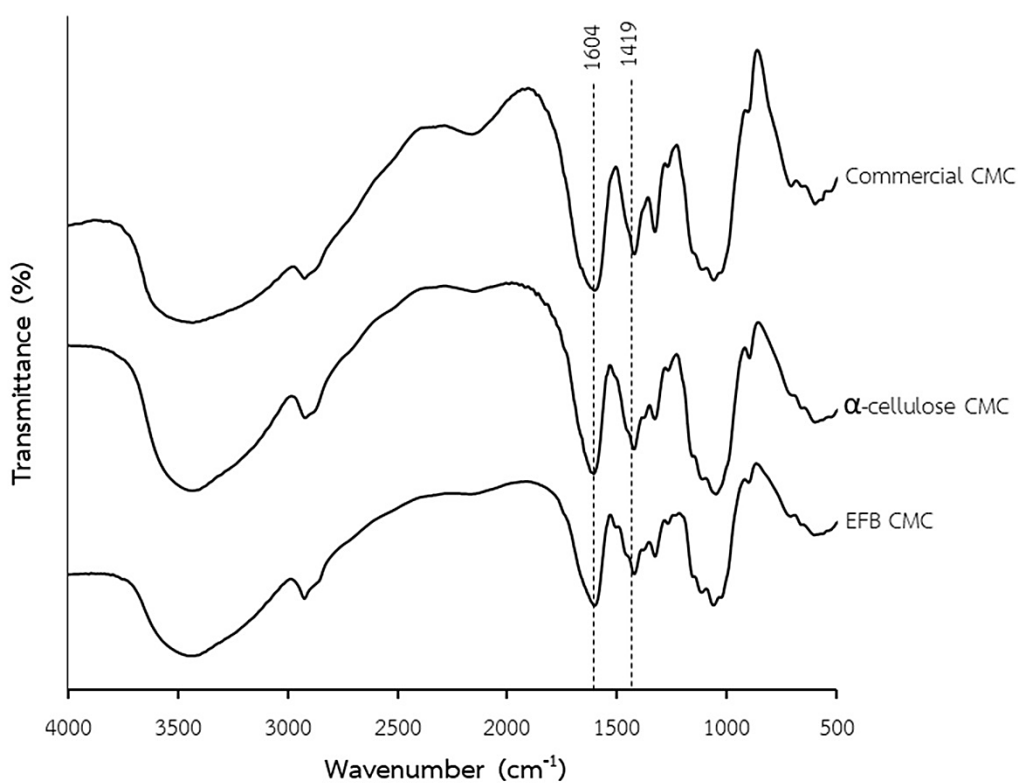
Figure 11 FTIR spectra of all CMC products.

4.1.3.4 Thermal analysis

Thermal properties of the prepared CMC products were determined using a thermogravimetric analysis (TGA). The TGA and Derivative thermogravimetric (DTG) curves are presented in Figure 12. It was first observed that water molecule was evaporated at the temperature ranging from 50°C to 150°C. Generally, all CMC products exhibited a single-step thermal degradation. Starting

decomposition (T_{onset}) of the commercial CMC occurred at the temperature of 263°C. This value was higher than the **α**-cellulose CMC (245°C) and EFB CMC (230°C), indicating that the commercial CMC was more thermal stable than the other synthesized CMCs. The maximum decomposition rate (T_{max}) was 301°C, 292°C, and 289°C for the commercial CMC, the **α**-cellulose CMC, and the EFB CMC, respectively. It can be observed that the EFB CMC reached lower T_{onset} and T_{max} in comparison with the commercial compounds. It was probably affected by residual lignin in the EFB CMC. The breakdown of **α**- and **β**-aryl-alkyl-ether bonds in lignin reportedly occurred at a lower temperature (150-300°C) (Monteiro et al., 2012). Thus, it contributed to a slight decline in T_{onset} and T_{max} value of the EFB CMC.
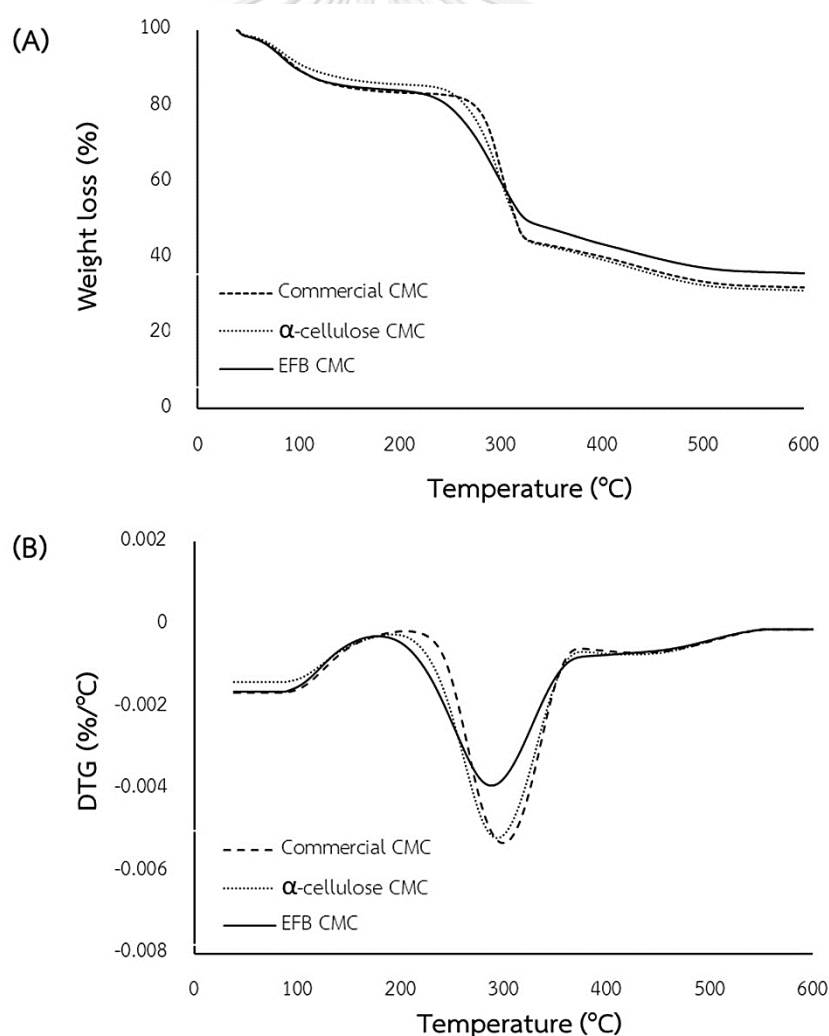
Figure 12 TGA (A) and DTG (B) curves of all CMC products.

4.2 Isolation and characterization of EFB lignin

      4.2.1 Purity and solubility

            The type of lignin used in this study was alkaline (soda) lignin since it was precipitated from the black liquor resulting from the alkaline extraction process. Thus, black liquor derived from alkaline extraction of the acid pretreated EFB pulp was chosen for lignin precipitation since it was also a part of the optimized extraction process for the most efficient EFB CMC synthesis. The yield of the extracted EFB lignin was 16.47 g/100 g EFB. The fact that the precipitated lignin yield was higher than the lignin content in the untreated EFB (14.97%) was likely due to the presence of co-precipitated carbohydrates such as cellulose, hemicellulose, and other extractives which were also detected by FTIR (Figure 13). Further measurement indicated that the EFB lignin purity was 64.39%. Interestingly, this value was higher than the previous study that reported that the purity of extracted EFB lignin extracted by methylene chloride, *n*-propanol, and methanol/methylene chloride were 41.6, 45.1, and 10.4%, respectively (Sun et al., 2000). Moreover, the extracted EFB lignin in this study was highly soluble in water (69.26%). This water-soluble ability suggested its potential to be blended with the EFB CMC for water-based composite film preparation.

      4.2.2 FTIR spectra

            FTIR spectroscopy was performed to determine the structure of the extracted EFB lignin (Figure 13). The peaks observed at 2924 and 2854 cm^{-1} corresponded to the C-H stretching vibrations from aliphatic groups (de Diego-Díaz et al., 2019). Aromatic skeletal vibrations (C=C) of the basic lignin structure were appeared at 1595 and 1419 cm^{-1} (Pinheiro et al., 2017). The peak at 1227 cm^{-1} could be attributed to the presence of phenolic -OH groups (Tan et al., 2019). The presence of carbohydrate as impurities in the extracted EFB lignin was detected due to the characteristic of C-O-C observed at 1049 cm^{-1} (Pinheiro et al., 2017).
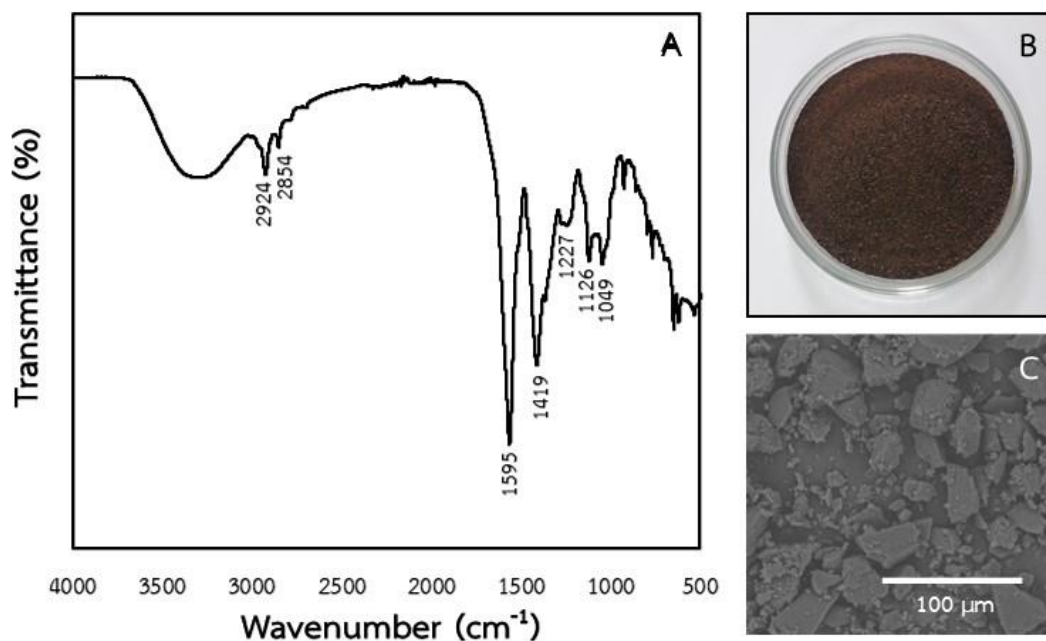
Figure 13 FTIR spectra (A), photographic image (B), and SEM image (C) of extracted EFB lignin.

4.2.3. Thermal analysis

The TGA and DTG curves of the extracted EFB lignin are presented in Figure 14. It was observed that evaporation of water molecule occurred at the temperature ranging from 50 to 150°C. Generally, the thermogravimetric profile of the extracted EFB lignin exhibited two-steps of degradation. The first step in the range of 150-350°C corresponded to the cleavage of α- and β-aryl-alkyl-ether linkages (Monteiro et al., 2012). In this step, the T_{max} value occurred at 314°C. Thus, the TGA curve also showed that more than 15% of the EFB lignin was degraded at this temperature. The last step, from 350 to 523°C, indicated the breakdown of lignin internal linkages, including the aromatic rings (Fernandes et al., 2021). This step reached the T_{max} value at 480°C. The last degradation of the EFB lignin (T_{end}) occurred at 523°C. Since this value indicated that the EFB lignin was more thermal stable than the EFB CMC (Figure 12), blending them together to form a composite film is also expected to improve the EFB CMC thermal stability.
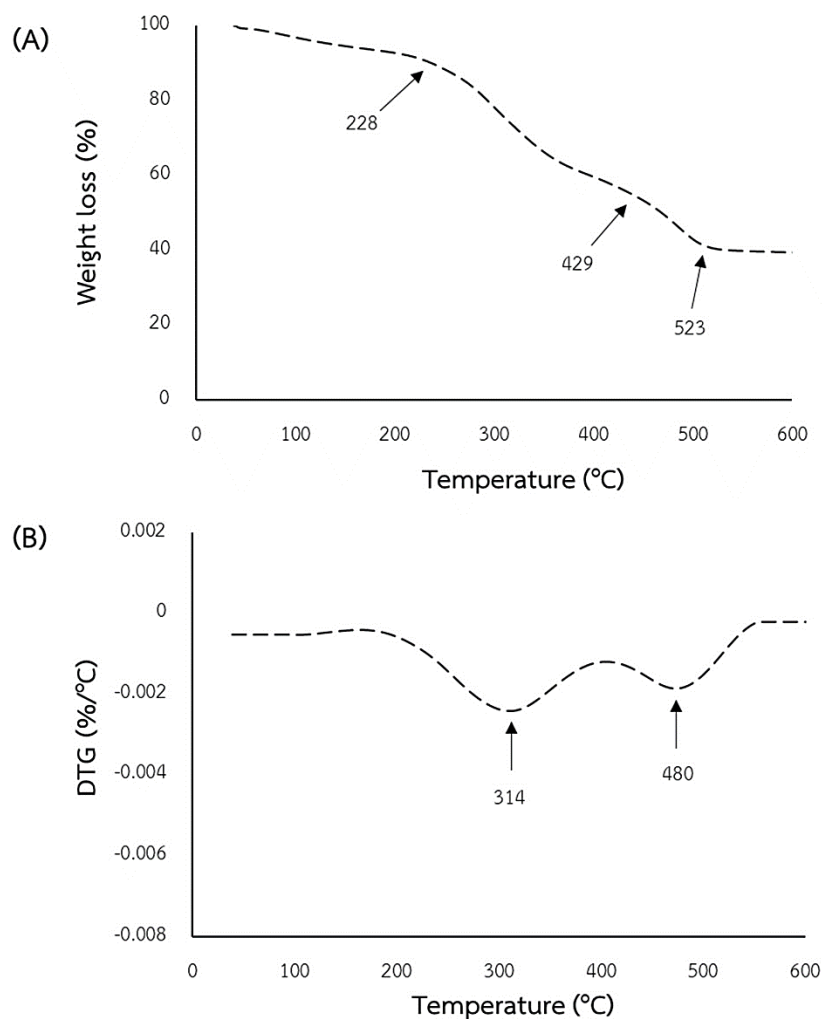
Figure 14 TGA (A) and DTG (B) of the extracted EFB lignin.

4.3 Film characterization

4.3.1 FTIR spectra

The FTIR spectra of the films were recorded at the wavenumber ranging from 4000 to 500 cm^{-1} (Figure 15). A sharp absorption peak observed at 3433 cm^{-1} presented the hydrogen-bonded-OH (Wu et al., 2011). The peak at 1635 cm^{-1} indicated the interaction of -COOH groups in CMC with -OH groups of glycerol (Yaradoddi et al., 2020). An increased EFB lignin incorporation into the EFB CMC film contributed to shift the wavenumber from 1419 cm^{-1} to 1466 cm^{-1} following by appearance of a new peak at 1388 cm^{-1}. Furthermore, the peaks detected at 1049 and 1119 cm^{-1} were related to the -O- stretching (Rachtanapun et al., 2012).
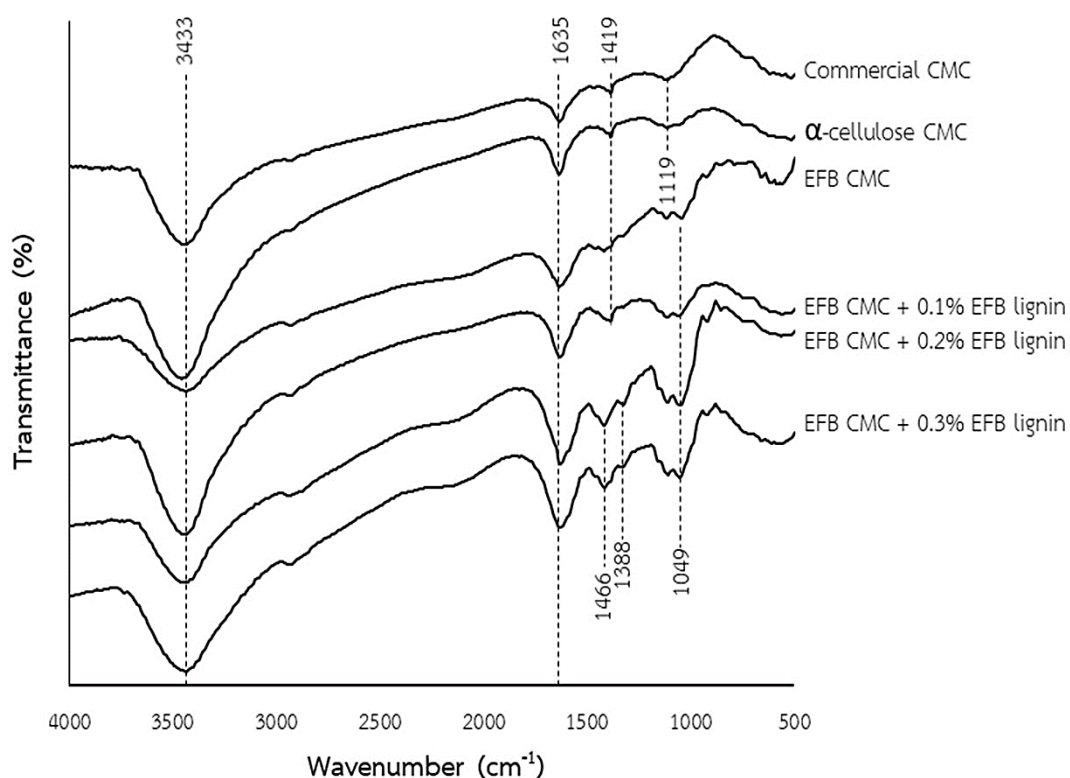
Figure 15 FTIR spectra of all CMC-based composite films.

4.3.2 Surface morphology

The scanning electron microscopy (SEM) images of the surface of all CMC-based films are shown in Figure 16. It was observed that the commercial CMC and the α-cellulose CMC had smooth and homogeneous surface. On the other hand, the surface of the EFB CMC was rough, probably due to the residual lignin content on the sample. When increasing the concentration of the EFB lignin, the slight physical changes were observed due to the presence of agglomerations. We concluded that the EFB lignin particles with an average size of 4.28 μm were not well dispersed. It demonstrated the low miscibility between the EFB CMC and EFB lignin. Some lignin particles could form hydrogen bonds among lignin itself via inter-molecular interaction. A similar situation has been reported by He et al. (2019) when acid modified commercial alkaline lignin nanoparticles (LNPs) were added into a polyvinyl alcohol (PVA) film.
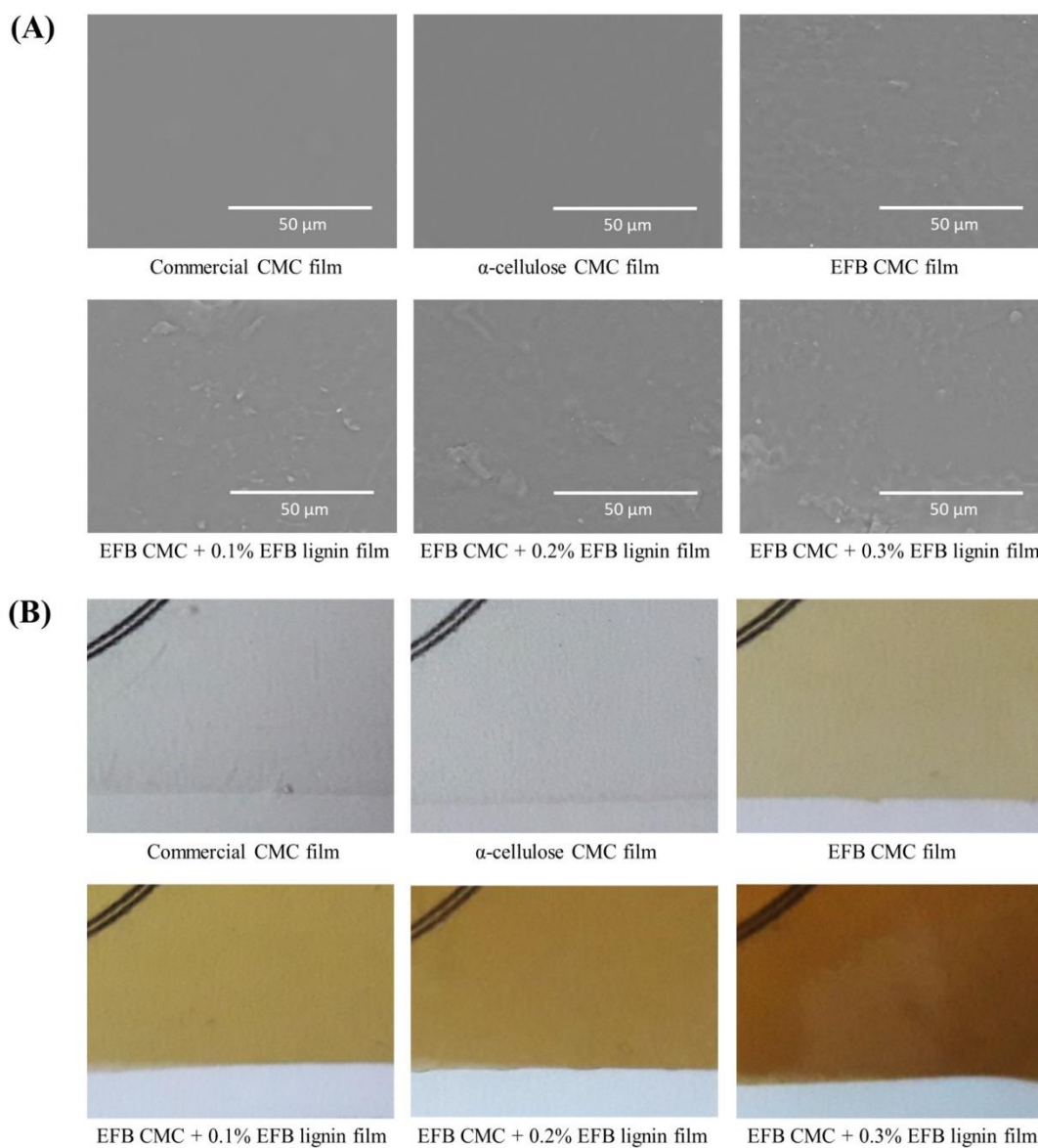
Figure 16 Scanning electron micrographs (A) and photographic images (B) of all CMC-based composite films. All composite films were placed on the lined paper background to show their transparency (B).

4.3.3 Color properties

Both the commercial CMC and the **α**-cellulose CMC exhibited a colorless film. However, the EFB CMC film was yellow in color affected by the

presence of residual lignin. Furthermore, an increase in EFB lignin incorporation significantly contributed to the color changes to become more reddish and yellowish in the EFB CMC-lignin composite films. It was evidenced by increased *a* and *b* values, respectively (Table 7). Moreover, an increase in the **ΔE** showed that the color was significantly different from the white standard. Although contributing to result in a dark color, incorporating EFB lignin improved the ability of the composite films to absorb UV-B (275-320 nm) and UV-A (320-380 nm) (Figure 19). Several authors have reported similar conditions (Izaguirre et al., 2020; Shankar and Rhim, 2017).

Table 6 Color properties of all CMC-based composite films.

No	Film	L^*	a^{**}	b^{***}	ΔE^{****}
1	Commercial CMC	3.13	0	0.29	3.22
2	**α**-cellulose CMC	1.47	0.11	0.01	1.48
3	EFB CMC	6.68	1.36	14.69	8.71
4	EFB CMC + 0.1% EFB lignin	13.33	0.71	27.69	15.28
5	EFB CMC + 0.2% EFB lignin	19.68	4.05	37.24	21.87
6	EFB CMC + 0.3% EFB lignin	39.85	14.89	53.6	43.78

*   Range of light to dark (0-100).

**   Red (positive) or green (negative).

***   Yellow (positive) or blue (negative).

****   Total color difference from a white standard.

4.3.4 Water contact angle

The surface wettability of the composite films was investigated by contact angle measurement. The results are presented in Table 8. A hydrophobic film possesses a contact angle value higher than 90° (Kiuru and Alakoski, 2004). In this study, all the prepared films were hydrophilic since they had contact angle values lower than 90°. It could be observed that the EFB CMC film had a contact angle of 63.3°. This value was significantly higher than the **α**-cellulose CMC film (46.0°). It was probably related to the surface roughness of the EFB CMC film

(Crouvisier-Urion et al., 2016). When 0.1% and 0.2% EFB lignin was added into the EFB CMC film, the contact angle values were reduced to 56.0^{o} and 53.3^{o}, respectively. Further excessive EFB lignin incorporation (0.3%) dramatically dropped the value to 42.0^{o}. We stated that the hydrophilic characteristic of EFB lignin strongly contributed to increasing hydrophilicity in the EFB CMC-lignin composite films. A similar situation has been reported by Zadeh et al. (2018), who reported that a soy protein isolate (SPI) film reduced its contact angle value after incorporating commercial alkali lignin and lignosulfonate.

4.3.5 Water vapor permeability

The water vapor permeability (WVP) represents the ability of a film to protect from the transmission of water vapor molecules through the film. Hence, a lower WVP value is desirable since it demonstrates a better property toward water vapor. In this study, the lowest WVP was achieved by the commercial CMC film with the value of 6.66×10^{-11} g m^{-1} s^{-1} Pa^{-1} (Table 8). This value was not significantly different compared to that WVP of the EFB CMC film (7.24×10^{-11} g m^{-1} s^{-1} Pa^{-1}). However, the α-cellulose CMC film revealed the highest WVP value (7.55×10^{-11} g m^{-1} s^{-1} Pa^{-1}), demonstrating its low performance in comparison to the commercial CMC film. Further, there was no significant change in WVP after the incorporation of EFB lignin at all concentrations. However, a slight acceleration in water diffusion was found when the EFB lignin addition increased. These phenomena were related to the strong hydrophilicity of the EFB lignin, whereby it could enhance the free hydroxyl groups in the EFB CMC-lignin composite films. Thus, they could easily interact with water vapor molecules. However, the amount of water vapor transmission across the films depends on the environmental conditions. An increase in relative humidity and temperature will enhance the water vapor permeability of the film (Chinma et al., 2015).

Table 7 Contact angle and WVP value of all CMC-based composite films.

No	Film	CA ($^{\circ}$)	WVP (x 10^{-11} g m^{-1} s^{-1} Pa^{-1})
1	Commercial CMC	ND*	6.66 ± 0.49^b
2	α-cellulose CMC	46.0 ± 1.7^c	7.55 ± 0.13^a
3	EFB CMC	63.3 ± 1.2^a	7.24 ± 0.39^{ab}
4	EFB CMC + 0.1% EFB lignin	56.0 ± 2.0^b	7.56 ± 0.39^a
5	EFB CMC + 0.2% EFB lignin	53.3 ± 2.3^b	7.68 ± 0.44^a
6	EFB CMC + 0.3% EFB lignin	42.0 ± 1.0^d	7.76 ± 0.30^a

* Not detectable, the film surface was sensitive when touching a drop of water.

Different superscript letters in the same column indicated significant different values at $p < 0.05$.

4.3.6 Thermal properties

The TGA was used to determine the thermal stability of the composite films. The bonds within the molecule of films were decomposed during the heating process in TGA (El-Sayed et al., 2011). As displayed in TGA and DTG curves, evaporation of water molecules in the films occurred at the temperature ranging from 50 to 150°C (Figure 17). The next stage was the volatilization of glycerol and dehydration of saccharide ring in CMC (Oun and Rhim, 2020; Suppiah et al., 2019). It could be observed that the second peak also appeared due to dihydroxylation and the pyrolytic fragmentation process in CMC (El-Sakhawy et al., 2019). The highest decomposition occurred in this stage, as shown from the T_{max} in the DTG curves. The last stage occurred above 400°C, which indicated oxidation and the breakdown of the residue from carbonaceous material (Roman and Winter, 2004).

Although a low T_{onset} demonstrated poor thermal stability of the EFB CMC film, Incorporating EFB lignin dramatically improved T_{onset} value as the EFB lignin concentration increased (Table 9). According to Avelino et al. (2019), lignin can act as a thermal stabilizer in polymeric films due to its richness in phenolic hydroxyl groups. Since EFB lignin was more thermal stable than EFB CMC, its addition could contribute to enhancing the thermal stability of the EFB CMC-lignin composite films. Due to the

incorporation of EFB lignin, the percentage of residue in the EFB CMC-lignin composite films was raised at the end of the heating process and dramatically reduced the total weight loss.
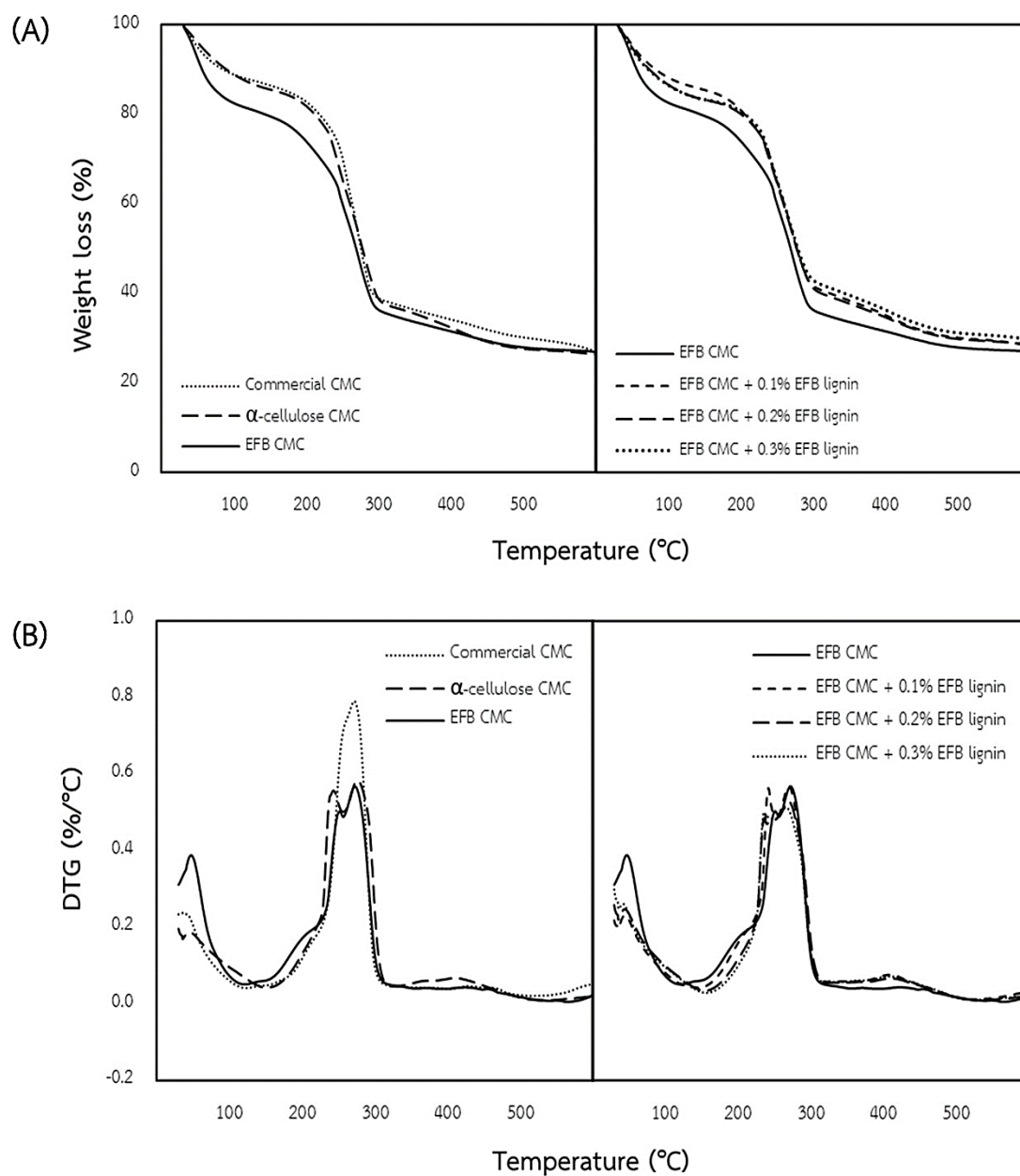
Figure 17 TGA (A) and DTG (B) curves of all CMC-based composite films.

Table 8 Thermal properties of all CMC-based composite films.

No	Film	T_{onset}* (°C)	T_{max}** (°C)	Weight loss (%)	Residue (%)
1	Commercial CMC	158.9	271.2	72.91	27.09
2	α-cellulose CMC	152.8	275.9	73.63	26.37
3	EFB CMC	124.5	272.6	73.08	26.92
4	EFB CMC + 0.1% EFB lignin	145.7	269.8	71.69	28.31
5	EFB CMC + 0.2% EFB lignin	145.9	269.6	71.48	28.52
6	EFB CMC + 0.3% EFB lignin	146.6	266.2	70.27	29.73

*   Temperature affecting the beginning decomposition of the film.

**   Temperature reaching maximum loss weight of the film.

4.3.7 Antioxidant activity

A radical scavenging (antioxidant) activity is also one of the important film properties since free radicals are hazardous to both biotic and abiotic entities. After reacting with film solutions, the decolorization of DPPH was noted as an indicator of antioxidant activity. It values of DPPH radical scavenging activity (RSA) and half-maximum inhibitory concentration (IC_{50}) are shown in Figure 18. It could be observed that the commercial CMC and the α-cellulose CMC films did not exhibit radical scavenging activity. These results were in line with the previous study by Michelin et al. (2020), who reported that a common commercial CMC film was not active against DPPH radicals. Interestingly, the EFB CMC film showed inhibition of the DPPH free radicals with an IC_{50} value of 10.34 mg mL^{-1}. The residual lignin on the EFB CMC film played an important role as a radical scavenger since it contained a richness in phenolic hydroxyl groups. As previously reported, it can react with free radicals by delivering proton and electron (Tian et al., 2017). When the EFB lignin was incorporated into the EFB CMC film, the radical scavenging activity was enhanced as the EFB lignin concentration increased. Thus, the decline of IC_{50} value indicated an improvement in the antioxidant activity. However, at a much higher concentration EFB lignin, an increase in antioxidant activity was not as sharp. Therefore, the EFB

CMC-lignin film loaded with 0.2% EFB lignin showed the highest antioxidant activity since it was not significantly different with 0.3% EFB lignin addition.
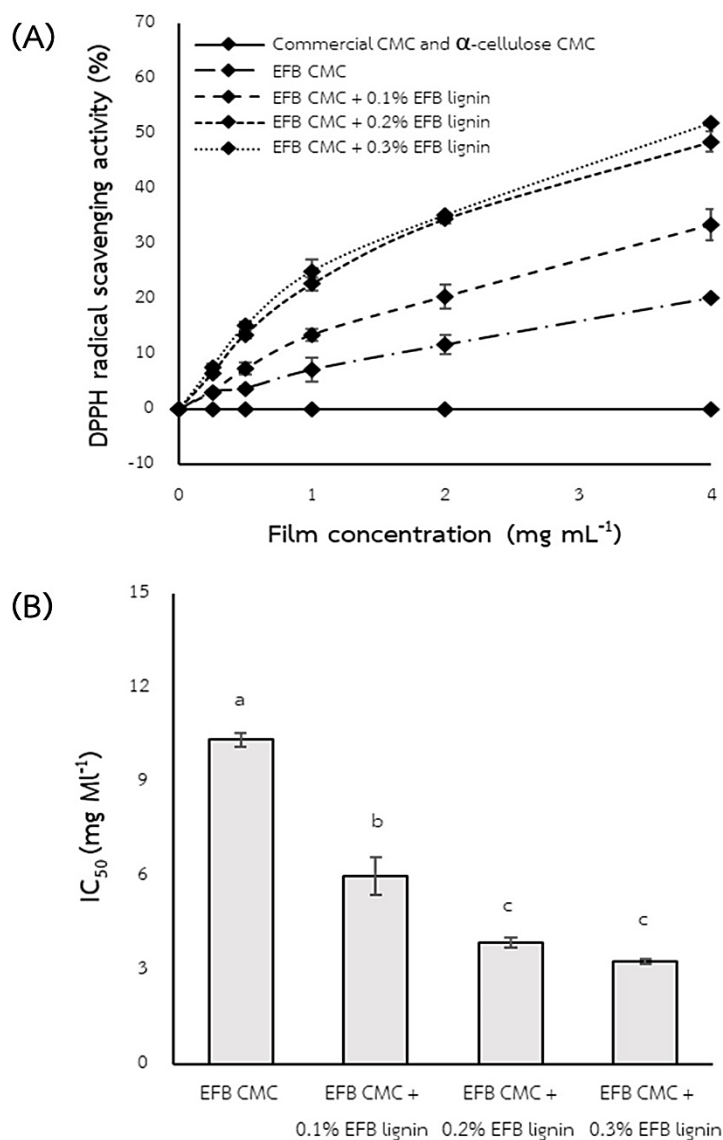
Figure 18 DPPH radical scavenging activity (A) and IC_{50} values (B) of all CMC-based composite films. Different superscript letters in the same graph indicated significant different values at $p < 0.05$.

Several works have reported the effect of lignin addition into various composite films to improve antioxidant activity. For instance, Avelino et al. (2019) investigated the influence of various soluble coconut shell lignin incorporation (1

wt%) on PMMA film and reported IC_{50} values of 27, 28, and 40 mg mL^{-1} for a PMMA-ACT-F film, PMMA-EtOH film, and PMMA-WCSAL film, respectively. A gelatin-Acacia lignin film revealed its highest antioxidant activity (67%) after incorporating lignin at a concentration of 40% (Aadil et al., 2016). A similar work about commercial CMC-corncob lignin film was previously reported by Michelin et al. (2020), who found that the CMC-lignin film achieved IC_{50} value at 50 μg_{lignin} mL^{-1}. In this study, the highest antioxidant activity of EFB CMC-lignin composite film completed IC_{50} at 3.27 mg mL^{-1}, or it was equivalent to the EFB lignin addition at 65 μg_{lignin} mL^{-1}. This finding demonstrated that the EFB lignin had a slightly lower antioxidant property. The carbohydrate residues as impurities in the EFB lignin might reduce its antioxidant properties since the polar groups of carbohydrates could form hydrogen bonds with the phenolic groups of lignin (Ugartondo et al., 2008). Similarly, a previous study reported that a high percentage of carbohydrates in the lignin complex could decrease its antiradical activity (Pei et al., 2020). Generally, a high existence of phenolic hydroxyl groups in lignin could improve the antioxidant potency (Guo et al., 2019). In the meanwhile, the presence of aliphatic hydroxyl groups exhibited a contrary result (He et al., 2019). However, it could be said that the EFB-CMC composite film is promising for active packaging film due to its antioxidant property.

4.3.8 UV-blocking capacity

The transmittance of all CMC-based composite films was recorded in the wavelength of 200 – 800 nm (Figure 19). The results demonstrated that the EFB CMC film exhibited a complete UV-B blocking with more than 90% UV-A blocking performance. On the other hand, the commercial CMC and the α-cellulose CMC films did not have this capacity. Again, it was noted that the residual lignin in the EFB CMC film significantly contributed to the absorption of UV. Further EFB lignin addition could lead to improve UV-A blocking ability. As shown in Figure 19, incorporation of 0.1% EFB lignin could bar almost all UV-A transmittance. The total UV-A and UV-B protection were obtained after increasing the EFB lignin addition up to 0.2% and 0.3%. Nevertheless, it also caused the reduction in transparency of the composite films. These results were consistent with the earlier study that reported that

incorporating lignin would improve UV-light absorption and reduce the transparency of cellulose-based film (Sadeghifar et al., 2017). In this study, considering that the excessive EFB lignin incorporation (0.3%) could decrease the film transparency, the EFB CMC-lignin composite film added with 0.2% EFB lignin was regarded as the optimal formula due to its effectiveness to block both UV-A and UV-B transmittance.
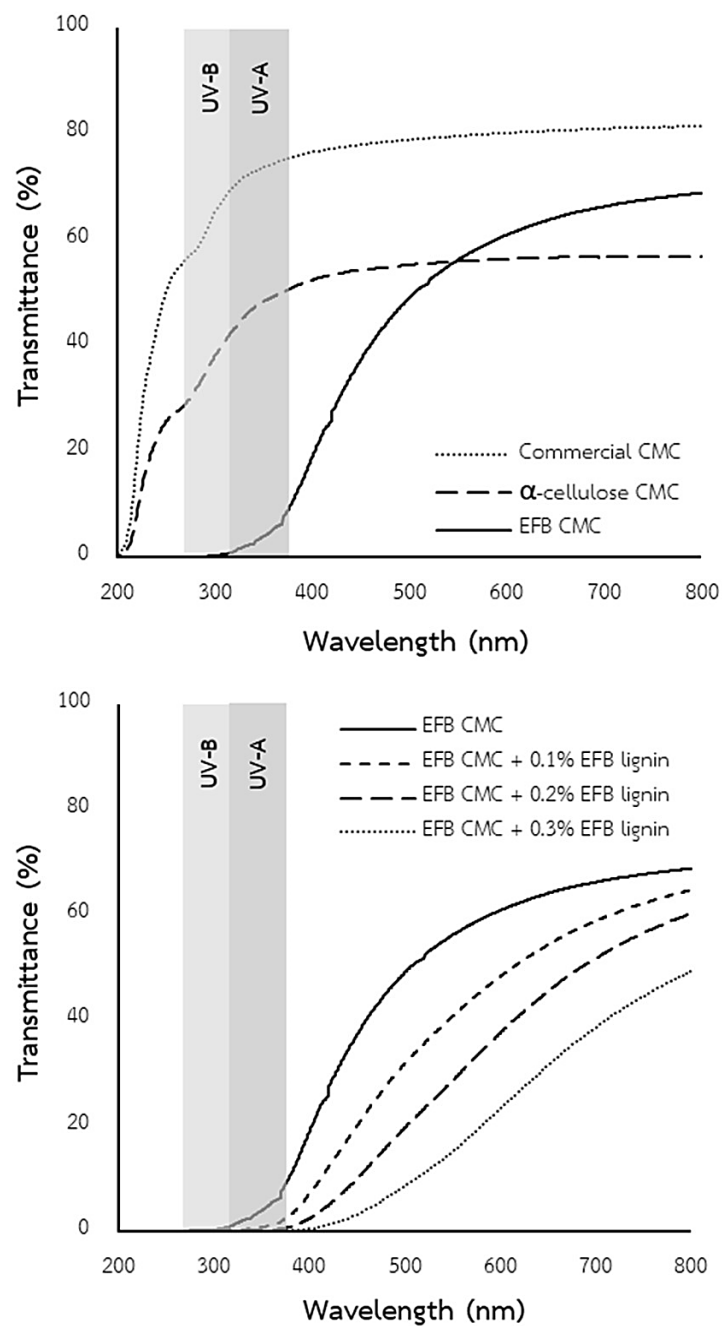

Figure 19 Transmittance profile of all CMC-based composite films.

Izaguirre et al. (2020) added various *Eucalyptus* lignin solutions dissolved in ethanol, methanol, ethyl acetate, and acetone into chitosan film and found that the UV transmittance of the obtained composite films dropped considerably. However, all UV regions were not totally absorbed at the lignin concentration tested. Sadeghifar et al. (2017) developed a composite film using commercial cellulose containing 2 wt% commercial kraft lignin that could block UV-B entirely and UV-A up to 90%. Similar to this study, a total UV-B blocking was found when commercial alkali and organosolv lignin at the concentration of 3 wt% were blended into a PVA film, whereas UV-A transmittance was still not absorbed totally (Posoknistakul et al., 2020). The complete UV-A and UV-B blocking capacity have been reported by Parit et al. (2018) after fabricating a cellulose nanocrystal (CNC) film with softwood kraft lignin at 10 wt%. A lower lignin concentration (commercial lignin nanomicelle) at 5 wt% (0.25% (w/v)) that could block all UV-transmittance through a PVA film was reported by Zhang et al. (2020). The UV blocking capacity of these aforementioned composite films were comparable with, if not inferior to, the EFB CMC-lignin composite film in this study that even at a lower concentration (0.2% (w/v)) of EFB lignin, it could completely block both UV-A and UV-B transmittance.

4.3.9 Thickness and mechanical properties

Thickness is one of the important parameters affecting film performance, such as barrier and mechanical properties (Mirzaei-Mohkam et al., 2020). In this study, the low standard deviation in the thickness assessment indicated the homogeneity of the film (Figure 20A). Furthermore, the thickness value of the EFB CMC film (54 μm) was in the middle between the commercial CMC film (47 μm) and the α-cellulose CMC film (60 μm). When the EFB lignin was incorporated at the concentrations of 0.1%, 0.2%, and 0.3%, the thickness of the EFB CMC-lignin composite film was increased to 55 μm, 57 μm, and 61 μm, respectively. These results were similar to the previous study that reported an increase in thickness of commercial CMC-based film after the addition of organosolv lignin (Michelin et al., 2020).
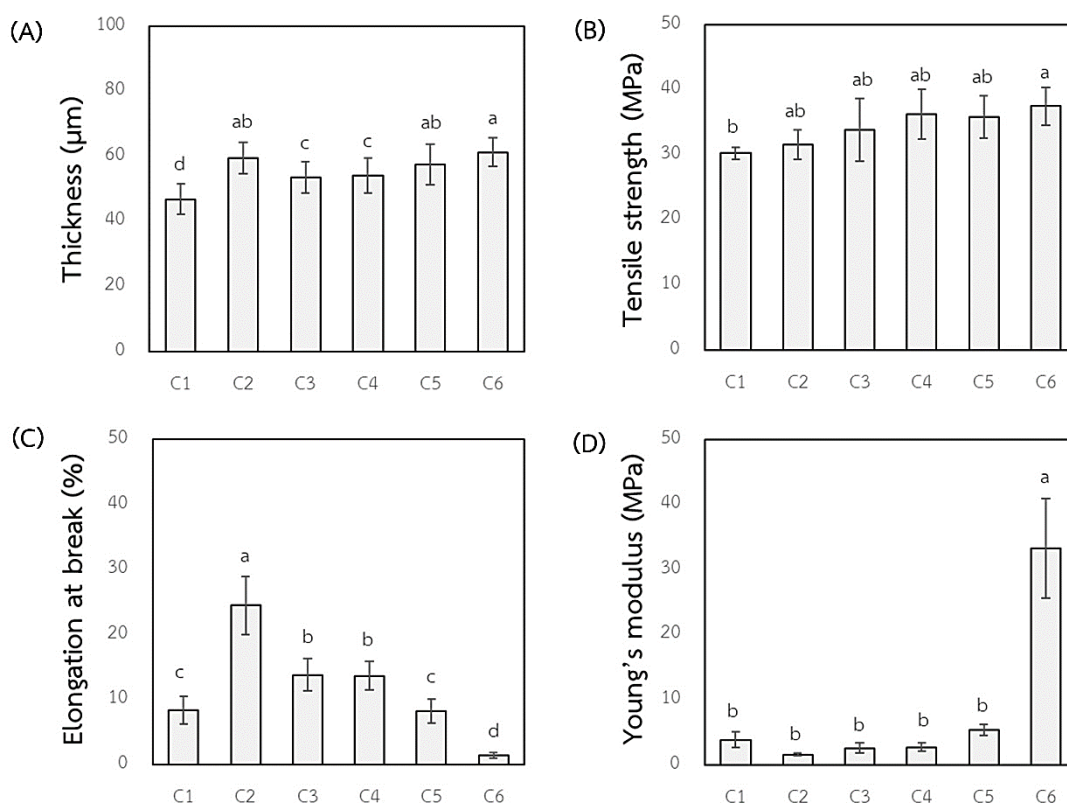
Figure 20 Thickness (A), tensile strength (B), elongation at break (C), and young's modulus (D) of CMC-based composite films: Commercial CMC film (C1), α-cellulose CMC film (C2), EFB CMC film (C3), EFB CMC film + 0.1% EFB lignin (C4), EFB CMC film + 0.2% EFB lignin (C5), and EFB CMC film + 0.3% EFB lignin (C6). Different letters indicated significant different values at $p < 0.05$.

In general, the films are commonly designed to hold stress during handling, shipping, and storage (Yang et al., 2016). Hence, the mechanical properties such as tensile strength (TS), elongation at break (EB), and young's modulus (YM) were assessed (Figure 20B-D). In term of the TS value, there was no significant difference between the commercial CMC film (30.27 MPa), the α-cellulose CMC film (31.56 MPa), and the EFB CMC film (33.87 MPa) (Figure 20B). A previous study reported that synthesized CMC from EFB cellulose resulted in a low TS compared to commercial compound (Amin et al., 2006). In this study, TS value of EFB CMC film was comparable with that of commercial CMC film. Thus, it also demonstrated that the method to synthesized EFB CMC in this study was successfully resulted in film

with superior mechanical strength. Moreover, the TS of the EFB CMC-lignin composite film was comparable to those of some conventional packaging films, such as high-density polyethylene (HDPE) (19-31 MPa), polystyrene (PS) (31-49 MPa), and polypropylene (PP) (27-98 MPa) (Yadav et al., 2020).

Among the EFB CMC, the commercial CMC, and the **α**-cellulose CMC films, the most significant difference was found in the elongation at break (EB) (Figure 20C). It was observed that the **α**-cellulose CMC film possessed the highest EB (24.74%), followed by the EFB CMC film (13.79%) and the commercial CMC film (8.33%). These obtained EB values were related to their DS, where higher carboxymethyl substituent will provide more inter-molecular interactions between the polymer chains (Rachtanapun et al., 2012). Furthermore, when the EFB lignin was added into the EFB CMC film, the EB value declined drastically, especially at the concentration of 0.3% (Figure 20). This phenomenon might be related to the presence of some agglomerations in the EFB CMC-lignin composite film surface. As previously reported, agglomerations can cause a premature rupture of the films; thus, it also contributes to decreasing the film elasticity (Kargarzadeh et al., 2020). A significant increase in Young's modulus (YM) of the EFB CMC-lignin composite film was also found after incorporating the maximum EFB lignin at 0.3% (w/v) (Figure 20D). However, a higher YM value is not desirable since it causes film stiffness (Lim, 2010). Therefore, these findings suggested that addition of the EFB lignin at a higher concentration than 0.2% (w/v) would increase film roughness and brittleness, which lead to unpreferable mechanical performance.

4.3.10 Biodegradability test

The film biodegradability is commonly affected by several factors, such as moisture content, weather conditions, microorganisms in the soil, and characteristic of the materials (film density and the presence of bioactive substances) (Nguyen et al., 2016). The biodegradability of all composite films was evaluated using soil burial test at ambient temperature. Since some organic materials in the soil were easily stuck on the film surface, weight loss measurement was difficult due to additional weight from those components. Therefore, morphological evaluation was

employed in this study. The breakage of the composite films into smaller pieces was noted as an indicator of the film's decomposition and a complete degradation was regarded when there was no visible piece of the film left. The biodegradation test was carried out for 6 weeks. The commercial CMC film was found to have the shortest degradation time (1 week), followed by the α-cellulose CMC film (2 weeks). The rapid degradation of the commercial CMC film might be related to its thickness which was thinner than the α-cellulose CMC film (Figure 20A). A previous study by Riaz et al. (2020) revealed that a commercial CMC film exhibited a weight loss of 58.14% after 3 weeks of burial in the soil. The much slower degradation was observed in the EFB CMC films (6 weeks) without and with additional lignin incorporation. It indicated that lignin played a role in biodegradation hindrance possibly through its antibacterial activity (Wang et al., 2021). Thus, it might affect the degradation time of the lignin-based composite film. All biodegradability tests in this study were a preliminary attempt to roughly determine the biodegradability of the films and the timeframe of which the significant change/degradation was apparent. Therefore, further in-depth experiments in which biological (microbes), chemical (organic and inorganic nutrients), and physical (soil type, pH, temperature, and moistures) factors are carefully required.

CHAPTER V

CONCLUSION

The biodegradable UV protection film was successfully prepared using cellulose and lignin extracted from EFB. The effective EFB cellulose isolation through alkaline extraction for subsequent CMC synthesis was enhanced by incorporating various chemical pretreatments and totally chlorine-free bleaching, which concluded that H_2SO_4 pretreatment-alkaline extraction-H_2O_2 bleaching step was considered the best protocol. Some physical characteristics of the EFB CMC film such as surface wettability, thickness, all mechanical properties, and water vapor permeability were comparable with films fabricated from commercial compounds. Surprisingly, the EFB CMC film had high antioxidant activity and total UV-B blocking capacity, while the EFB lignin addition at the concentration of 0.2% into it could contribute to reach the highest antioxidant activity and total UV-A and UV-B blocking performance. The antioxidant activity and UV protection capacity of the EFB CMC-lignin composite film will promise its application in the active transparent food packaging to replace traditional packaging made from polyester film, glass, or metal. This study promotes a straightforward method to valorize the otherwise unprofitable EFB waste for commercial process development in the future, especially to produce a biodegradable UV protection packaging film.

REFERENCES

Aadil, K.R., Barapatre, A. and Jha, H. 2016. Synthesis and characterization of Acacia lignin-gelatin film for its possible application in food packaging. *Bioresources & Bioprocessing*, 3, 1-11.

Abdel-Hamid, A.M., Solbiati, J.O. and Cann, I.K. 2013. Insights into lignin degradation and its potential industrial applications. *Advances in Applied Microbiology*, 82, 1-28.

Abnisa, F. and Daud, W.M.A.W. 2014. A review on co-pyrolysis of biomass: an optional technique to obtain a high-grade pyrolysis oil. *Energy Conversion Management*, 87, 71-85.

Ahmad, F.B., Zhang, Z., Doherty, W.O. and O'Hara, I.M. 2016. Evaluation of oil production from oil palm empty fruit bunch by oleaginous micro-organisms. *Biofuels, Bioproducts and Biorefining*, 10, 378-392.

Ahmad, F.B., Zhang, Z., Doherty, W.O. and O'Hara, I.M. 2019. The outlook of the production of advanced fuels and chemicals from integrated oil palm biomass biorefinery. *Renewable and Sustainable Energy Reviews*, 109, 386-411.

Akhtar, J., Teo, C.L., Lai, L.W., Hassan, N., Idris, A. and Aziz, R.A. 2015. Factors affecting delignification of oil palm empty fruit bunch by microwave-assisted dilute acid/alkali pretreatment. *BioResources*, 10, 588-596.

Almutawa, F., Vandal, R., Wang, S.Q. and Lim, H.W. 2013. Current status of photoprotection by window glass, automobile glass, window films, and sunglasses. *Photodermatology, Photoimmunology & Photomedicine*, 29, 65-72.

Amin, M.C.I., Soom, R., Ahmad, I. and Lian, H.H. 2006. Carboxymethyl Cellulose From Palm Oil Empty Fruit Bunch–Their Properties And Use As A Film Coating Agent. *Jurnal Sains Kesihatan Malaysia*, 4, 53-62.

An, S., Li, W., Xue, F., Li, X., Xia, Y., Liu, Q., Chen, L., Jameel, H. and Chang, H.-m. 2020. Effect of removing hemicellulose and lignin synchronously under mild conditions on enzymatic hydrolysis of corn stover. *Fuel Processing Technology*, 204, 106407.

Asl, S.A., Mousavi, M. and Labbafi, M. 2017. Synthesis and characterization of carboxymethyl cellulose from sugarcane bagasse. *Journal of Food Processing and*

Technology, 8,

Avelino, F., de Oliveira, D.R., Mazzetto, S.E. and Lomonaco, D. 2019. Poly (methyl methacrylate) films reinforced with coconut shell lignin fractions to enhance their UV-blocking, antioxidant and thermo-mechanical properties. *International Journal of Biological Macromolecules*, 125, 171-180.

Barakat, A., de Vries, H. and Rouau, X. 2013. Dry fractionation process as an important step in current and future lignocellulose biorefineries: a review. *Bioresource Technology*, 134, 362-373.

Barba, C., Montané, D., Rinaudo, M. and Farriol, X. 2002. Synthesis and characterization of carboxymethylcelluloses (CMC) from non-wood fibers I. Accessibility of cellulose fibers and CMC synthesis. *Cellulose*, 9, 319-326.

Benítez, A. and Walther, A. 2017. Cellulose nanofibril nanopapers and bioinspired nanocomposites: a review to understand the mechanical property space. *Journal of Materials Chemistry A*, 5, 16003-16024.

Bhandari, P.N., Jones, D.D. and Hanna, M.A. 2012. Carboxymethylation of cellulose using reactive extrusion. *Carbohydrate Polymers*, 87, 2246-2254.

Bhat, R., Abdullah, N., Din, R.H. and Tay, G.-S. 2013. Producing novel sago starch based food packaging films by incorporating lignin isolated from oil palm black liquor waste. *Journal of Food Engineering*, 119, 707-713.

Bian, H., Chen, L., Dong, M., Wang, L., Wang, R., Zhou, X., Wu, C., Wang, X., Ji, X. and Dai, H. 2021. Natural lignocellulosic nanofibril film with excellent ultraviolet blocking performance and robust environment resistance. *International Journal of Biological Macromolecules*, 166, 1578-1585.

Brethauer, S. and Wyman, C.E. 2010. Continuous hydrolysis and fermentation for cellulosic ethanol production. *Bioresource Technology*, 101, 4862-4874.

Candido, R. and Gonçalves, A. 2016. Synthesis of cellulose acetate and carboxymethylcellulose from sugarcane straw. *Carbohydrate Polymers*, 152, 679-686.

Carter, C., Finley, W., Fry, J., Jackson, D. and Willis, L. 2007. Palm oil markets and future supply. *European Journal of Lipid Science and Technology*, 109, 307-314.

Casaburi, A., Rojo, Ú.M., Cerrutti, P., Vázquez, A. and Foresti, M.L. 2018. Carboxymethyl

cellulose with tailored degree of substitution obtained from bacterial cellulose. *Food Hydrocolloids*, 75, 147-156.

Cazón, P., Velázquez, G. and Vázquez, M. 2019. Characterization of bacterial cellulose films combined with chitosan and polyvinyl alcohol: Evaluation of mechanical and barrier properties. *Carbohydrate polymers*, 216, 72-85.

Chakar, F.S. and Ragauskas, A.J. 2004. Review of current and future softwood kraft lignin process chemistry. *Industrial Crops and Products*, 20, 131-141.

Chang, S.H. 2014. An overview of empty fruit bunch from oil palm as feedstock for bio-oil production. *Biomass and Bioenergy*, 62, 174-181.

Chen, J., Adjallé, K., Lai, T.T., Barnabé, S., Perrier, M. and Paris, J. 2020. Effect of mechanical pretreatment for enzymatic hydrolysis of woody residues, corn Stover and alfalfa. *Waste and Biomass Valorization*, 11, 5847-5856.

Ching, Y.C. and Ng, T.S. 2014. Effect of preparation conditions on cellulose from oil palm empty fruit bunch fiber. *BioResources*, 9, 6373-6385.

Chinma, C., Ariahu, C. and Alakali, J. 2015. Effect of temperature and relative humidity on the water vapour permeability and mechanical properties of cassava starch and soy protein concentrate based edible films. *Journal of Food Science & Technology*, 52, 2380-2386.

Chio, C., Sain, M. and Qin, W. 2019. Lignin utilization: a review of lignin depolymerization from various aspects. *Renewable and Sustainable Energy Reviews*, 107, 232-249.

Chua, K.Y., Azzahari, A.D., Abouloula, C.N., Sonsudin, F., Shahabudin, N. and Yahya, R. 2020. Cellulose-based polymer electrolyte derived from waste coconut husk: residual lignin as a natural plasticizer. *Journal of Polymer Research*, 27, 1-14.

Corley, R. and Tinker, P. 2003. The climate and soils of the oil palm-growing regions. *The Oil Palm, Fourth Edition. Blackwell Science Ltd, Oxford, United Kingdom*, 53-88.

Crouvisier-Urion, K., Bodart, P.R., Winckler, P., Raya, J.s., Gougeon, R.g.D., Cayot, P., Domenek, S., Debeaufort, F.d.r. and Karbowiak, T. 2016. Biobased composite films from chitosan and lignin: antioxidant activity related to structure and moisture. *ACS Sustainable Chemistry & Engineering*, 4, 6371-6381.

Dahnum, D., Tasum, S.O., Triwahyuni, E., Nurdin, M. and Abimanyu, H. 2015. Comparison

of SHF and SSF processes using enzyme and dry yeast for optimization of bioethanol production from empty fruit bunch. *Energy Procedia*, 68, 107-116.

de Dicastillo, C.L., Bustos, F., Guarda, A. and Galotto, M.J. 2016. Cross-linked methyl cellulose films with murta fruit extract for antioxidant and antimicrobial active food packaging. *Food Hydrocolloids*, 60, 335-344.

de Diego-Díaz, B., Duran, A., Álvarez-García, M.R. and Fernández-Rodríguez, J. 2019. New trends in physicochemical characterization of solid lignocellulosic waste in anaerobic digestion. *Fuel*, 245, 240-246.

Dislich, C., Keyel, A.C., Salecker, J., Kisel, Y., Meyer, K.M., Auliya, M., Barnes, A.D., Corre, M.D., Darras, K. and Faust, H. 2017. A review of the ecosystem functions in oil palm plantations, using forests as a reference system. *Biological Reviews*, 92, 1539-1569.

Dos Santos, R.M., Neto, W.P.F., Silvério, H.A., Martins, D.F., Dantas, N.O. and Pasquini, D. 2013. Cellulose nanocrystals from pineapple leaf, a new approach for the reuse of this agro-waste. *Industrial Crops and Products*, 50, 707-714.

El-Sakhawy, M., Tohamy, H.-A.S., Salama, A. and Kamel, S. 2019. Thermal properties of carboxymethyl cellulose acetate butyrate. *Cellulose Chemistry & Technology*, 53, 667-675.

El-Sayed, S., Mahmoud, K., Fatah, A. and Hassen, A. 2011. DSC, TGA and dielectric properties of carboxymethyl cellulose/polyvinyl alcohol blends. *Physica B: Condensed Matter*, 406, 4068-4076.

Fernandes, C., Melro, E., Magalhães, S., Alves, L., Craveiro, R., Filipe, A., Valente, A.J., Martins, G., Antunes, F.E. and Romano, A. 2021. New deep eutectic solvent assisted extraction of highly pure lignin from maritime pine sawdust (Pinus pinaster). *International Journal of Biological Macromolecules*,

Fernández-Rodríguez, J., Gordobil, O., Robles, E., González-Alriols, M. and Labidi, J. 2017. Lignin valorization from side-streams produced during agricultural waste pulping and total chlorine free bleaching. *Journal of Cleaner Production*, 142, 2609-2617.

Gan, L., Zhou, M., Yang, D. and Qiu, X. 2013. Preparation and evaluation of carboxymethylated lignin as dispersant for aqueous graphite suspension using

Turbiscan Lab analyzer. *Journal of Dispersion Science and Technology*, 34, 644-650.

Garcia-Nunez, J.A., Ramirez-Contreras, N.E., Rodriguez, D.T., Silva-Lora, E., Frear, C.S., Stockle, C. and Garcia-Perez, M. 2016. Evolution of palm oil mills into bio-refineries: Literature review on current and potential uses of residual biomass and effluents. *Resources, Conservation and Recycling*, 110, 99-114.

Geng, W., Venditti, R.A., Pawlak, J.J. and Chang, H.-m. 2018. Effect of delignification on hemicellulose extraction from switchgrass, poplar, and pine and its effect on enzymatic convertibility of cellulose-rich residues. *BioResources*, 13, 4946-4963.

Gerlock, J., Kucherov, A. and Smith, C. 2001. Determination of active HALS in automotive paint systems II: HALS distribution in weathered clearcoat/basecoat paint systems. *Polymer Degradation and Stability*, 73, 201-210.

Goering, H.K. and Van Soest, P.J. 1970. *Forage fiber analyses (apparatus, reagents, procedures, and some applications)*, US Agricultural Research Service,

Golbaghi, L., Khamforoush, M. and Hatami, T. 2017. Carboxymethyl cellulose production from sugarcane bagasse with steam explosion pulping: Experimental, modeling, and optimization. *Carbohydrate Polymers*, 174, 780-788.

Gourichon, H. 2019. Analysis of incentives and disincentives for palm oil in Nigeria. *Gates Open Research*, 3, 11-36.

Guo, Y., Tian, D., Shen, F., Yang, G., Long, L., He, J., Song, C., Zhang, J., Zhu, Y. and Huang, C. 2019. Transparent cellulose/technical lignin composite films for advanced packaging. *Polymers*, 11, 1455.

Haldar, D. and Purkait, M.K. 2020. Thermochemical pretreatment enhanced bioconversion of elephant grass (Pennisetum purpureum): insight on the production of sugars and lignin. *Biomass Conversion and Biorefinery*, 1-14.

Haleem, N., Arshad, M., Shahid, M. and Tahir, M.A. 2014. Synthesis of carboxymethyl cellulose from waste of cotton ginning industry. *Carbohydrate Polymers*, 113, 249-255.

Hamawand, I., Seneweera, S., Kumarasinghe, P. and Bundschuh, J. 2020. Nanoparticle technology for separation of cellulose, hemicellulose and lignin nanoparticles from lignocellulose biomass: A short review. *Nano-Structures & Nano-Objects*, 24,

100601.

Han, Y., Yu, M. and Wang, L. 2018. Physical and antimicrobial properties of sodium alginate/carboxymethyl cellulose films incorporated with cinnamon essential oil. *Food Packaging and Shelf Life*, 15, 35-42.

He, B., Wang, W., Song, Y., Ou, Y. and Zhu, J. 2020. Structural and physical properties of carboxymethyl cellulose/gelatin films functionalized with antioxidant of bamboo leaves. *International Journal of Biological Macromolecules*, 164, 1649-1656.

He, X., Luzi, F., Hao, X., Yang, W., Torre, L., Xiao, Z., Xie, Y. and Puglia, D. 2019. Thermal, antioxidant and swelling behaviour of transparent polyvinyl (alcohol) films in presence of hydrophobic citric acid-modified lignin nanoparticles. *International Journal of Biological Macromolecules*, 127, 665-676.

Herrera, M., Thitiwutthisakul, K., Yang, X., Rujitanaroj, P.-o., Rojas, R. and Berglund, L. 2018. Preparation and evaluation of high-lignin content cellulose nanofibrils from eucalyptus pulp. *Cellulose*, 25, 3121-3133.

Horodytska, O., Valdés, F.J. and Fullana, A. 2018. Plastic flexible films waste management–A state of art review. *Waste Management*, 77, 413-425.

Hossain, M.A., Phung, T.K., Rahaman, M.S., Tulaphol, S., Jasinski, J.B. and Sathitsuksanoh, N. 2019. Catalytic cleavage of the β-O-4 aryl ether bonds of lignin model compounds by Ru/C catalyst. *Applied Catalysis A: General*, 582, 117100.

Huang, C., Dong, H., Zhang, Z., Bian, H. and Yong, Q. 2020. Procuring the nano-scale lignin in prehydrolyzate as ingredient to prepare cellulose nanofibril composite film with multiple functions. *Cellulose*, 27, 9355-9370.

Huang, C., Sun, R., Chang, H.-m., Yong, Q., Jameel, H. and Phillips, R. 2019. Production of dissolving grade pulp from tobacco stalk through SO2-ethanol-water fractionation, alkaline extraction, and bleaching processes. *Bioresources*, 14, 5544-5558.

Itoh, H., Wada, M., Honda, Y., Kuwahara, M. and Watanabe, T. 2003. Bioorganosolve pretreatments for simultaneous saccharification and fermentation of beech wood by ethanolysis and white rot fungi. *Journal of Biotechnology*, 103, 273-280.

Izaguirre, N., Gordobil, O., Robles, E. and Labidi, J. 2020. Enhancement of UV absorbance and mechanical properties of chitosan films by the incorporation of

solvolytically fractionated lignins. *International Journal of Biological Macromolecules*, 155, 447-455.

Jha, P. 2020. Effect of plasticizer and antimicrobial agents on functional properties of bionanocomposite films based on corn starch-chitosan for food packaging applications. *International Journal of Biological Macromolecules*, 160, 571-582.

Jiang, B., Yu, J., Luo, X., Zhu, Y. and Jin, Y. 2018. A strategy to improve enzymatic saccharification of wheat straw by adding water-soluble lignin prepared from alkali pretreatment spent liquor. *Process Biochemistry*, 71, 147-151.

Jiang, G., Hou, X., Zeng, X., Zhang, C., Wu, H., Shen, G., Li, S., Luo, Q., Li, M. and Liu, X. 2020. Preparation and characterization of indicator films from carboxymethyl-cellulose/starch and purple sweet potato (Ipomoea batatas (L.) lam) anthocyanins for monitoring fish freshness. *International Journal of Biological Macromolecules*, 143, 359-372.

Jiang, Y., Zhou, J., Zhang, Q., Zhao, G., Heng, L., Chen, D. and Liu, D. 2017. Preparation of cellulose nanocrystals from Humulus japonicus stem and the influence of high temperature pretreatment. *Carbohydrate Polymers*, 164, 284-293.

Joshi, G., Naithani, S., Varshney, V., Bisht, S.S., Rana, V. and Gupta, P. 2015. Synthesis and characterization of carboxymethyl cellulose from office waste paper: a greener approach towards waste management. *Waste Management*, 38, 33-40.

Jouki, M., Khazaei, N., Ghasemlou, M. and HadiNezhad, M. 2013. Effect of glycerol concentration on edible film production from cress seed carbohydrate gum. *Carbohydrate Polymers*, 96, 39-46.

Kai, D., Tan, M.J., Chee, P.L., Chua, Y.K., Yap, Y.L. and Loh, X.J. 2016. Towards lignin-based functional materials in a sustainable world. *Green Chemistry*, 18, 1175-1200.

Kargarzadeh, H., Galeski, A. and Pawlak, A. 2020. PBAT green composites: Effects of kraft lignin particles on the morphological, thermal, crystalline, macro and micromechanical properties. *Polymer*, 203, 122748.

Kazzaz, A.E., Feizi, Z.H. and Fatehi, P. 2019. Grafting strategies for hydroxy groups of lignin for producing materials. *Green Chemistry*, 21, 5714-5752.

Kim, G.-H. and Um, B.-H. 2020. Fractionation and characterization of lignins from

Miscanthus via organosolv and soda pulping for biorefinery applications. *International Journal of Biological Macromolecules*, 158, 443-451.

Kiuru, M. and Alakoski, E. 2004. Low sliding angles in hydrophobic and oleophobic coatings prepared with plasma discharge method. *Materials Letters*, 58, 2213-2216.

Klemm, D., Heublein, B., Fink, H.P. and Bohn, A. 2005. Cellulose: fascinating biopolymer and sustainable raw material. *Angewandte Chemie International Edition*, 44, 3358-3393.

Kolibaba, T.J., Stevens, D.L., Pangburn, S.T., Condassamy, O., Camus, M., Grau, E. and Grunlan, J.C. 2020. UV-protection from chitosan derivatized lignin multilayer thin film. *RSC Advances*, 10, 32959-32965.

Konduri, M.K., Kong, F. and Fatehi, P. 2015. Production of carboxymethylated lignin and its application as a dispersant. *European Polymer Journal*, 70, 371-383.

Kullavanijaya, P. and Lim, H.W. 2005. Photoprotection. *Journal of the American Academy of Dermatology*, 52, 937-958.

Kumar, A.K. and Sharma, S. 2017. Recent updates on different methods of pretreatment of lignocellulosic feedstocks: a review. *Bioresources and Bioprocessing*, 4, 1-19.

Lakshmi, D.S., Trivedi, N. and Reddy, C. 2017. Synthesis and characterization of seaweed cellulose derived carboxymethyl cellulose. *Carbohydrate Polymers*, 157, 1604-1610.

Lambert, P.F., Münger, K., Rösl, F., Hasche, D. and Tommasino, M. 2020. Beta human papillomaviruses and skin cancer. *Nature*, 588, E20-E21.

Lan, W., Zhang, R., Ji, T., Sameen, D.E., Ahmed, S., Qin, W., Dai, J., He, L. and Liu, Y. 2020. Improving nisin production by encapsulated Lactococcus lactis with starch/carboxymethyl cellulose edible films. *Carbohydrate Polymers*, 251, 117062.

Laser, M., Larson, E., Dale, B., Wang, M., Greene, N. and Lynd, L.R. 2009. Comparative analysis of efficiency, environmental impact, and process economics for mature biomass refining scenarios. *Biofuels, Bioproducts and Biorefining*, 3, 247-270.

Lee, J., Mahendra, S. and Alvarez, P.J. 2010. Nanomaterials in the construction industry: a review of their applications and environmental health and safety

considerations. *ACS Nano*, 4, 3580-3590.

Li, H., Shi, H., He, Y., Fei, X. and Peng, L. 2020a. Preparation and characterization of carboxymethyl cellulose-based composite films reinforced by cellulose nanocrystals derived from pea hull waste for food packaging applications. *International Journal of Biological Macromolecules*, 164, 4104-4112.

Li, X., Zhang, X., Yao, S., Chang, H., Wang, Y. and Zhang, Z. 2020b. UV-blocking, transparent and hazy cellulose nanopaper with superior strength based on varied components of poplar mechanical pulp. *Cellulose*, 27, 6563-6576.

Lim, C.W. 2010. Is a nanorod (or nanotube) with a lower Young's modulus stiffer? Is not Young's modulus a stiffness indicator? *Science China Physics, Mechanics & Astronomy*, 53, 712-724.

Liu, W.-J., Jiang, H. and Yu, H.-Q. 2015. Thermochemical conversion of lignin to functional materials: a review and future directions. *Green Chemistry*, 17, 4888-4907.

Liu, W., Chen, W., Hou, Q., Wang, S. and Liu, F. 2018. Effects of combined pretreatment of dilute acid pre-extraction and chemical-assisted mechanical refining on enzymatic hydrolysis of lignocellulosic biomass. *RSC Advances*, 8, 10207-10214.

Louis, A.C.F. and Venkatachalam, S. 2020. Energy efficient process for valorization of corn cob as a source for nanocrystalline cellulose and hemicellulose production. *International Journal of Biological Macromolecules*, 163, 260-269.

Mahmood, N., Yuan, Z., Schmidt, J. and Xu, C.C. 2016. Depolymerization of lignins and their applications for the preparation of polyols and rigid polyurethane foams: A review. *Renewable and Sustainable Energy Reviews*, 60, 317-329.

Martins, M., Dinamarco, T.M. and Goldbeck, R. 2020. Recombinant chimeric enzymes for lignocellulosic biomass hydrolysis. *Enzyme and Microbial Technology*, 109647.

Mba, O.I., Dumont, M.-J. and Ngadi, M. 2015. Palm oil: Processing, characterization and utilization in the food industry–A review. *Food Bioscience*, 10, 26-41.

Michelin, M., Marques, A.M., Pastrana, L.M., Teixeira, J.A. and Cerqueira, M.A. 2020. Carboxymethyl cellulose-based films: Effect of organosolv lignin incorporation on physicochemical and antioxidant properties. *Journal of Food Engineering*, 285, 110107.

Mirzaei-Mohkam, A., Garavand, F., Dehnad, D., Keramat, J. and Nasirpour, A. 2020. Physical, mechanical, thermal and structural characteristics of nanoencapsulated vitamin E loaded carboxymethyl cellulose films. *Progress in Organic Coatings*, 138, 105383.

Mittal, A., Katahira, R., Himmel, M.E. and Johnson, D.K. 2011. Effects of alkaline or liquid-ammonia treatment on crystalline cellulose: changes in crystalline structure and effects on enzymatic digestibility. *Biotechnology for Biofuels*, 4, 1-16.

Monteiro, S.N., Calado, V., Margem, F.M. and Rodriguez, R.J. 2012. Thermogravimetric stability behavior of less common lignocellulosic fibers-a review. *Journal of Materials Research and Technology*, 1, 189-199.

Moussa, I., Khiari, R., Moussa, A., Belgacem, M.N. and Mhenni, M.F. 2019. Preparation and characterization of carboxymethyl cellulose with a high degree of substitution from agricultural wastes. *Fibers and Polymers*, 20, 933-943.

Nadeem, H., Naseri, M., Shanmugam, K., Dehghani, M., Browne, C., Miri, S., Garnier, G. and Batchelor, W. 2020. An energy efficient production of high moisture barrier nanocellulose/carboxymethyl cellulose films via spray-deposition technique. *Carbohydrate Polymers*, 250, 116911.

Naidu, D.S., Hlangothi, S.P. and John, M.J. 2018. Bio-based products from xylan: A review. *Carbohydrate Polymers*, 179, 28-41.

Naseem, A., Tabasum, S., Zia, K.M., Zuber, M., Ali, M. and Noreen, A. 2016. Lignin-derivatives based polymers, blends and composites: A review. *International Journal of Biological Macromolecules*, 93, 296-313.

Ndaba, B., Roopnarain, A., Daramola, M.O. and Adeleke, R. 2020. Influence of extraction methods on antimicrobial activities of lignin-based materials: a review. *Sustainable Chemistry and Pharmacy*, 18, 100342.

Nguyen, D.M., Do, T.V.V., Grillet, A.-C., Thuc, H.H. and Thuc, C.N.H. 2016. Biodegradability of polymer film based on low density polyethylene and cassava starch. *International Biodeterioration & Biodegradation*, 115, 257-265.

Oh, Y., Park, S., Jung, D., Oh, K.K. and Lee, S.H. 2020. Effect of hydrogen bond donor on the choline chloride-based deep eutectic solvent-mediated extraction of lignin from pine wood. *International Journal of Biological Macromolecules*, 165, 187-

197.

Oun, A.A. and Rhim, J.-W. 2015. Preparation and characterization of sodium carboxymethyl cellulose/cotton linter cellulose nanofibril composite films. *Carbohydrate Polymers*, 127, 101-109.

Oun, A.A. and Rhim, J.-W. 2020. Preparation of multifunctional carboxymethyl cellulose-based films incorporated with chitin nanocrystal and grapefruit seed extract. *International Journal of Biological Macromolecules*, 152, 1038-1046.

Pang, J., Liu, X., Zhang, X., Wu, Y. and Sun, R. 2013. Fabrication of cellulose film with enhanced mechanical properties in ionic liquid 1-allyl-3-methylimidaxolium chloride (AmimCl). *Materials*, 6, 1270-1284.

Parid, D.M., Abd Rahman, N.A., Baharuddin, A.S., Mohammed, M.A.P., Johari, A.M. and Razak, S.Z.A. 2018. Synthesis and characterization of carboxymethyl cellulose from oil palm empty fruit bunch stalk fibres. *BioResources*, 13, 535-554.

Parit, M., Saha, P., Davis, V.A. and Jiang, Z. 2018. Transparent and homogenous cellulose nanocrystal/lignin UV-protection films. *ACS Omega*, 3, 10679-10691.

Park, S., Baker, J.O., Himmel, M.E., Parilla, P.A. and Johnson, D.K. 2010. Cellulose crystallinity index: measurement techniques and their impact on interpreting cellulase performance. *Biotechnology for Biofuels*, 3, 1-10.

Park, S.H. and Kim, S.H. 2014. Poly (ethylene terephthalate) recycling for high value added textiles. *Fashion and Textiles*, 1, 1-17.

Park, S.Y., Kim, J.-Y., Youn, H.J. and Choi, J.W. 2019. Utilization of lignin fractions in UV resistant lignin-PLA biocomposites via lignin-lactide grafting. *International Journal of Biological Macromolecules*, 138, 1029-1034.

Patinvoh, R.J., Osadolor, O.A., Chandolias, K., Horváth, I.S and Taherzadeh, M.J. 2017. Innovative pretreatment strategies for biogas production. *Bioresource Technology*, 224, 13-24.

Pei, W., Chen, Z.S., Chan, H.Y.E., Zheng, L., Liang, C. and Huang, C. 2020. Isolation and Identification of a Novel Anti-protein Aggregation Activity of Lignin-Carbohydrate Complex From Chionanthus retusus Leaves. *Frontiers in Bioengineering & Biotechnology*, 8,

Philippini, R.R., Martiniano, S.E., Chandel, A.K., de Carvalho, W. and da Silva, S.S. 2019.

Pretreatment of sugarcane bagasse from cane hybrids: effects on chemical composition and 2G sugars recovery. *Waste and Biomass Valorization*, 10, 1561-1570.

Pinheiro, F.G.C., Soares, A.K.L., Santaella, S.T., e Silva, L.M.A., Canuto, K.M., Cáceres, C.A., de Freitas Rosa, M., de Andrade Feitosa, J.P. and Leitão, R.C. 2017. Optimization of the acetosolv extraction of lignin from sugarcane bagasse for phenolic resin production. *Industrial Crops and Products*, 96, 80-90.

Posoknistakul, P., Tangkrakul, C., Chaosuanphae, P., Deepentham, S., Techasawong, W., Phonphirunrot, N., Bairak, S., Sakdaronnarong, C. and Laosiripojana, N. 2020. Fabrication and Characterization of Lignin Particles and Their Ultraviolet Protection Ability in PVA Composite Film. *ACS Omega*, 5, 20976-20982.

Qi, X.-M., Liu, S.-Y., Chu, F.-B., Pang, S., Liang, Y.-R., Guan, Y., Peng, F. and Sun, R.-C. 2016. Preparation and characterization of blended films from quaternized hemicelluloses and carboxymethyl cellulose. *Materials*, 9, 4.

Rachtanapun, P., Luangkamin, S., Tanprasert, K. and Suriyatem, R. 2012. Carboxymethyl cellulose film from durian rind. *LWT-Food Science & Technology*, 48, 52-58.

Rahman, A.A., Abdullah, N. and Sulaiman, F. 2014. Temperature effect on the characterization of pyrolysis products from oil palm fronds. *Advances in Energy Engineering*, 2, 14-21.

Rahmi, Lelifajri, Julinawati and Shabrina 2017. Preparation of chitosan composite film reinforced with cellulose isolated from oil palm empty fruit bunch and application in cadmium ions removal from aqueous solutions. *Carbohydrate Polymers*, 170, 226-233.

Riaz, A., Lagnika, C., Luo, H., Nie, M., Dai, Z., Liu, C., Abdin, M., Hashim, M.M., Li, D. and Song, J. 2020. Effect of Chinese chives (Allium tuberosum) addition to carboxymethyl cellulose based food packaging films. *Carbohydrate polymers*, 235, 115944.

Richardson, S. and Gorton, L. 2003. Characterisation of the substituent distribution in starch and cellulose derivatives. *Analytica Chimica Acta*, 497, 27-65.

Roberts, J.E. 2011. Ultraviolet radiation as a risk factor for cataract and macular degeneration. *Eye & Contact Lens*, 37, 246-249.

Rodsamran, P. and Sothornvit, R. 2017. Rice stubble as a new biopolymer source to produce carboxymethyl cellulose-blended films. *Carbohydrate Polymers*, 171, 94-101.

Roman, M. and Winter, W.T. 2004. Effect of sulfate groups from sulfuric acid hydrolysis on the thermal degradation behavior of bacterial cellulose. *Biomacromolecules*, 5, 1671-1677.

Rorrer, N.A., Nicholson, S., Carpenter, A., Biddy, M.J., Grundl, N.J. and Beckham, G.T. 2019. Combining reclaimed PET with bio-based monomers enables plastics upcycling. *Joule*, 3, 1006-1027.

Sadeghifar, H. and Ragauskas, A. 2020. Lignin as a UV light blocker—a review. *Polymers*, 12, 1134.

Sadeghifar, H., Venditti, R., Jur, J., Gorga, R.E. and Pawlak, J.J. 2017. Cellulose-lignin biodegradable and flexible UV protection film. *ACS Sustainable Chemistry & Engineering*, 5, 625-631.

Saito, K., Horikawa, Y., Sugiyama, J., Watanabe, T., Kobayashi, Y. and Takabe, K. 2016. Effect of thermochemical pretreatment on lignin alteration and cell wall microstructural degradation in Eucalyptus globulus: comparison of acid, alkali, and water pretreatments. *Journal of Wood Science*, 62, 276-284.

Santos, R.B., Hart, P., Jameel, H. and Chang, H.-m. 2013. Wood based lignin reactions important to the biorefinery and pulp and paper industries. *BioResources*, 8, 1456-1477.

Shankar, S. and Rhim, J.-W. 2017. Preparation and characterization of agar/lignin/silver nanoparticles composite films with ultraviolet light barrier and antibacterial properties. *Food Hydrocolloids*, 71, 76-84.

Shankar, S., Wang, L.-F. and Rhim, J.-W. 2019. Effect of melanin nanoparticles on the mechanical, water vapor barrier, and antioxidant properties of gelatin-based films for food packaging application. *Food Packaging and Shelf Life*, 21, 100363.

Shui, T., Feng, S., Chen, G., Li, A., Yuan, Z., Shui, H., Kuboki, T. and Xu, C. 2017. Synthesis of sodium carboxymethyl cellulose using bleached crude cellulose fractionated from cornstalk. *Biomass and Bioenergy*, 105, 51-58.

Sidik, D.A.B., Ngadi, N. and Amin, N.A.S. 2013. Optimization of lignin production from

empty fruit bunch via liquefaction with ionic liquid. *Bioresource Technology*, 135, 690-696.

Sigler, M. 2014. The effects of plastic pollution on aquatic wildlife: current situations and future solutions. *Water, Air, and Soil Pollution*, 225, 1-9.

Singh, N., Hui, D., Singh, R., Ahuja, I., Feo, L. and Fraternali, F. 2017. Recycling of plastic solid waste: A state of art review and future applications. *Composites Part B: Engineering*, 115, 409-422.

Sirviö, J.A., Ismail, M.Y., Zhang, K., Tejesvi, M.V. and Ämmälä, A. 2020. Transparent lignin-containing wood nanofiber films with UV-blocking, oxygen barrier, and anti-microbial properties. *Journal of Materials Chemistry A*, 8, 7935-7946.

Sudiyani, Y., Styarini, D., Triwahyuni, E., Sembiring, K.C., Aristiawan, Y., Abimanyu, H. and Han, M.H. 2013. Utilization of biomass waste empty fruit bunch fiber of palm oil for bioethanol production using pilot–scale unit. *Energy Procedia*, 32, 31-38.

Sukiran, M.A., Abnisa, F., Daud, W.M.A.W., Bakar, N.A. and Loh, S.K. 2017. A review of torrefaction of oil palm solid wastes for biofuel production. *Energy Conversion and Management*, 149, 101-120.

Sulaiman, F., Abdullah, N., Gerhauser, H. and Shariff, A. 2010. A perspective of oil palm and its wastes. *Journal of Physical Science*, 21, 67-77.

Sun, R., Tomkinson, J. and Jones, G.L. 2000. Fractional characterization of ash-AQ lignin by successive extraction with organic solvents from oil palm EFB fibre. *Polymer Degradation and Stability*, 68, 111-119.

Suppiah, K., Leng, T.P., Husseinsyah, S., Rahman, R., Keat, Y.C. and Heng, C. 2019. Thermal properties of carboxymethyl cellulose (CMC) filled halloysite nanotube (HNT) bio-nanocomposite films. *Materials Today: Proceedings*, 16, 1611-1616.

Syaftika, N. and Matsumura, Y. 2018. Comparative study of hydrothermal pretreatment for rice straw and its corresponding mixture of cellulose, xylan, and lignin. *Bioresource Technology*, 255, 1-6.

Tan, X., Zhang, Q., Wang, W., Zhuang, X., Deng, Y. and Yuan, Z. 2019. Comparison study of organosolv pretreatment on hybrid pennisetum for enzymatic saccharification and lignin isolation. *Fuel*, 249, 334-340.

Tang, P.L., Hassan, O., Yue, C.S. and Abdul, P.M. 2020. Lignin extraction from oil palm

empty fruit bunch fiber (OPEFBF) via different alkaline treatments. *Biomass Conversion and Biorefinery*, 10, 125-138.

Taniguchi, I., Yoshida, S., Hiraga, K., Miyamoto, K., Kimura, Y. and Oda, K. 2019. Biodegradation of PET: current status and application aspects. *ACS Catalysis*, 9, 4089-4105.

Tarasov, D., Leitch, M. and Fatehi, P. 2018. Lignin–carbohydrate complexes: properties, applications, analyses, and methods of extraction: a review. *Biotechnology for Biofuels*, 11, 1-28.

Teow, Y.H., Amirudin, S.N. and Ho, K.C. 2020. Sustainable approach to the synthesis of cellulose membrane from oil palm empty fruit bunch for dye wastewater treatment. *Journal of Water Process Engineering*, 34, 101182.

Tian, D., Hu, J., Bao, J., Chandra, R.P., Saddler, J.N. and Lu, C. 2017. Lignin valorization: Lignin nanoparticles as high-value bio-additive for multifunctional nanocomposites. *Biotechnology for Biofuels*, 10, 1-11.

Tian, S.-Q., Zhao, R.-Y. and Chen, Z.-C. 2018. Review of the pretreatment and bioconversion of lignocellulosic biomass from wheat straw materials. *Renewable and Sustainable Energy Reviews*, 91, 483-489.

Trache, D., Hussin, M.H., Chuin, C.T.H., Sabar, S., Fazita, M.N., Taiwo, O.F., Hassan, T. and Haafiz, M.M. 2016. Microcrystalline cellulose: Isolation, characterization and bio-composites application—A review. *International Journal of Biological Macromolecules*, 93, 789-804.

Tribot, A., Amer, G., Alio, M.A., de Baynast, H., Delattre, C., Pons, A., Mathias, J.-D., Callois, J.-M., Vial, C. and Michaud, P. 2019. Wood-lignin: Supply, extraction processes and use as bio-based material. *European Polymer Journal*, 112, 228-240.

Ugartondo, V., Mitjans, M. and Vinardell, M.P. 2008. Comparative antioxidant and cytotoxic effects of lignins from different sources. *Bioresource Technology*, 99, 6683-6687.

Ünlü, C.H. 2013. Carboxymethylcellulose from recycled newspaper in aqueous medium. *Carbohydrate Polymers*, 97, 159-164.

Vena, P., García-Aparicio, M., Brienzo, M., Görgens, J. and Rypstra, T. 2013. Impact of

hemicelluloses pre-extraction on pulp properties of sugarcane bagasse. *Journal of Cellulose Chemistry and Technology*, 47, 425-441.

Verma, R., Vinoda, K., Papireddy, M. and Gowda, A. 2016. Toxic pollutants from plastic waste-a review. *Procedia Environmental Sciences*, 35, 701-708.

Vilela, C., Pinto, R.J., Coelho, J., Domingues, M.R., Daina, S., Sadocco, P., Santos, S.A. and Freire, C.S. 2017. Bioactive chitosan/ellagic acid films with UV-light protection for active food packaging. *Food Hydrocolloids*, 73, 120-128.

Volynets, B., Ein-Mozaffari, F. and Dahman, Y. 2017. Biomass processing into ethanol: pretreatment, enzymatic hydrolysis, fermentation, rheology, and mixing. *Green Processing and Synthesis*, 6, 1-22.

Wang, F., Zhang, Q., Li, X., Huang, K., Shao, W., Yao, D. and Huang, C. 2019. Redox-responsive blend hydrogel films based on carboxymethyl cellulose/chitosan microspheres as dual delivery carrier. *International Journal of Biological Macromolecules*, 134, 413-421.

Wang, H., Gurau, G. and Rogers, R.D. 2012. Ionic liquid processing of cellulose. *Chemical Society Reviews*, 41, 1519-1537.

Wang, Y., Wang, H., Li, Z., Yang, D., Qiu, X., Liu, Y., Yan, M. and Li, Q. 2021. Fabrication of litchi-like lignin/zinc oxide composites with enhanced antibacterial activity and their application in polyurethane films. *Journal of Colloid and Interface Science*,

Waring, M. and Parsons, D. 2001. Physico-chemical characterisation of carboxymethylated spun cellulose fibres. *Biomaterials*, 22, 903-912.

Weerasooriya, P., Nadhilah, R., Owolabi, F., Hashim, R., Khalil, H.A., Syahariza, Z., Hussin, M., Hiziroglu, S. and Haafiz, M. 2020. Exploring the properties of hemicellulose based carboxymethyl cellulose film as a potential green packaging. *Current Research in Green Sustainable Chemistry*, 1, 20-28.

Wei, Z., Cai, C., Huang, Y., Wang, P., Song, J., Deng, L. and Fu, Y. 2020. Strong biodegradable cellulose materials with improved crystallinity via hydrogen bonding tailoring strategy for UV blocking and antioxidant activity. *International Journal of Biological Macromolecules*, 164, 27-36.

Wu, D., Chang, P.R. and Ma, X. 2011. Preparation and properties of layered double hydroxide–carboxymethylcellulose sodium/glycerol plasticized starch

nanocomposites. *Carbohydrate Polymers*, 86, 877-882.

Wu, W., Liu, T., Deng, X., Sun, Q., Cao, X., Feng, Y., Wang, B., Roy, V.A. and Li, R.K. 2019. Ecofriendly UV-protective films based on poly (propylene carbonate) biocomposites filled with TiO2 decorated lignin. *International Journal of Biological Macromolecules*, 126, 1030-1036.

Xing, Q., Ruch, D., Dubois, P., Wu, L. and Wang, W.-J. 2017. Biodegradable and high-performance poly (butylene adipate-co-terephthalate)–lignin UV-blocking films. *ACS Sustainable Chemistry & Engineering*, 5, 10342-10351.

Xu, Y.-H., Zhou, Q., Li, M.-F., Bian, J. and Peng, F. 2019. Tetrahydro-2-furanmethanol pretreatment of eucalyptus to enhance cellulose enzymatic hydrolysis and to produce high-quality lignin. *Bioresource Technology*, 280, 489-492.

Yadav, M., Behera, K., Chang, Y.-H. and Chiu, F.-C. 2020. Cellulose nanocrystal reinforced chitosan based uv barrier composite films for sustainable packaging. *Polymers*, 12, 202.

Yang, H., Zhang, X., Luo, H., Liu, B., Shiga, T.M., Li, X., Im Kim, J., Rubinelli, P., Overton, J.C. and Subramanyam, V. 2019. Overcoming cellulose recalcitrance in woody biomass for the lignin-first biorefinery. *Biotechnology for Biofuels*, 12, 1-18.

Yang, J., Wu, L., Yang, H. and Pan, Y. 2021a. Using the Major Components (Cellulose, Hemicellulose, and Lignin) of Phyllostachys praecox Bamboo Shoot as Dietary Fiber. *Frontiers in Bioengineering and Biotechnology*, 9, 239.

Yang, W., Ding, H., Qi, G., Li, C., Xu, P., Zheng, T., Zhu, X., Kenny, J.M., Puglia, D. and Ma, P. 2021b. Highly transparent PVA/nanolignin composite films with excellent UV shielding, antibacterial and antioxidant performance. *Reactive and Functional Polymers*, 162, 104873.

Yang, W., Owczarek, J., Fortunati, E., Kozanecki, M., Mazzaglia, A., Balestra, G., Kenny, J., Torre, L. and Puglia, D. 2016. Antioxidant and antibacterial lignin nanoparticles in polyvinyl alcohol/chitosan films for active packaging. *Industrial Crops and Products*, 94, 800-811.

Yaradoddi, J.S., Banapurmath, N.R., Ganachari, S.V., Soudagar, M.E.M., Mubarak, N., Hallad, S., Hugar, S. and Fayaz, H. 2020. Biodegradable carboxymethyl cellulose based material for sustainable packaging application. *Scientific Reports*, 10, 1-13.

Yu, J., Paterson, N., Blamey, J. and Millan, M. 2017. Cellulose, xylan and lignin interactions during pyrolysis of lignocellulosic biomass. *Fuel*, 191, 140-149.

Zabihollahi, N., Alizadeh, A., Almasi, H., Hanifian, S. and Hamishekar, H. 2020. Development and characterization of carboxymethyl cellulose based probiotic nanocomposite film containing cellulose nanofiber and inulin for chicken fillet shelf life extension. *International Journal of Biological Macromolecules*, 160, 409-417.

Zadeh, E.M., O'Keefe, S.F. and Kim, Y.-T. 2018. Utilization of lignin in biopolymeric packaging films. *ACS omega*, 3, 7388-7398.

Zailuddin, N.L.I. and Husseinsyah, S. 2016. Tensile properties and morphology of oil palm empty fruit bunch regenerated cellulose biocomposite films. *Procedia Chemistry*, 19, 366-372.

Zakaria, S.M., Idris, A., Chandrasekaram, K. and Alias, Y. 2020. Efficiency of bronsted acidic ionic liquids in the dissolution and depolymerization of lignin from rice husk into high value-added products. *Industrial Crops and Products*, 157, 112885.

Zayat, M., Garcia-Parejo, P. and Levy, D. 2007. Preventing UV-light damage of light sensitive materials using a highly protective UV-absorbing coating. *Chemical Society Reviews*, 36, 1270-1281.

Zhang, C., Wen, H., Chen, C., Cai, D., Fu, C., Li, P., Qin, P. and Tan, T. 2019. Simultaneous saccharification and juice co-fermentation for high-titer ethanol production using sweet sorghum stalk. *Renewable Energy*, 134, 44-53.

Zhang, X., Liu, W., Liu, W. and Qiu, X. 2020. High performance PVA/lignin nanocomposite films with excellent water vapor barrier and UV-shielding properties. *International Journal of Biological Macromolecules*, 142, 551-558.

APPENDIX

LIST OF TABLES AND FIGURES (APPENDIX)

Table A1 Searching the optimized condition for EFB CMC-based film prior to EFB lignin addition.

No	Conditions			Thickness (mm)	Tensile strength (Mpa)	Elongation at Break (%)	UV-B (%)	UV-A (%)
	EFB CMC concentration (%)	Total solution (mL)	Glycerol concentration (%)					
1	2.0	30	0.50	0.066 ± 0.01^c	8.48 ± 1.29^b	31.33 ± 4.05^c	ND	ND
2	2.5	30	0.50	0.088 ± 0.00^b	20.85 ± 2.28^a	20.86 ± 3.56^c	ND	ND
3	3.0	30	0.50	0.099 ± 0.01^a	20.23 ± 1.72^a	11.99 ± 4.01^a	ND	ND
4	2.5	25	0.50	0.068 ± 0.01^a	25.33 ± 1.15^b	14.64 ± 061^{ns}	6.02	0.00
5	2.5	20	0.50	0.054 ± 0.01^b	33.87 ± 4.80^a	13.79 ± 2.50^{ns}	9.75	0.00
6	2.5	15	0.50	0.043 ± 0.01^c	35.42 ± 2.79^a	13.79 ± 1.21^{ns}	10.41	0.87
7	2.5	20	0.00	0.047 ± 0.00^e	48.47 ± 1.67^a	2.04 ± 0.81^d	8.32	0.00
8	2.5	20	0.25	0.052 ± 0.00^d	40.60 ± 4.13^b	2.58 ± 0.32^d	9.65	0.00
9*	2.5	20	0.50	0.054 ± 0.01^d	33.87 ± 4.80^c	13.79 ± 2.50^c	9.75	0.00
10	2.5	20	0.75	0.061 ± 0.01^c	26.00 ± 2.49^d	16.88 ± 3.88^c	12.39	1.48
11	2.5	20	1.00	0.067 ± 0.01^b	15.08 ± 2.98^e	33.80 ± 3.75^b	17.96	2.80
12	2.5	20	1.25	0.077 ± 0.00^a	10.05 ± 1.33^a	40.62 ± 3.69^a	19.35	3.25

* Optimized composition of the EFB CMC film according to its preferable mechanical performances and complete UV-B blocking.

Different subscribed letters in the same section indicated the significant different at $p < 0.05$ in DMRT.

Figure A1 The brittle characteristic of EFB CMC films due to low glycerol concentration (less than 0.50% v/v).

Figure A2 Effect of high glycerol concentration (more than 0.50% v/v) in the EFB CMC films on their sensitive surface (sticky).
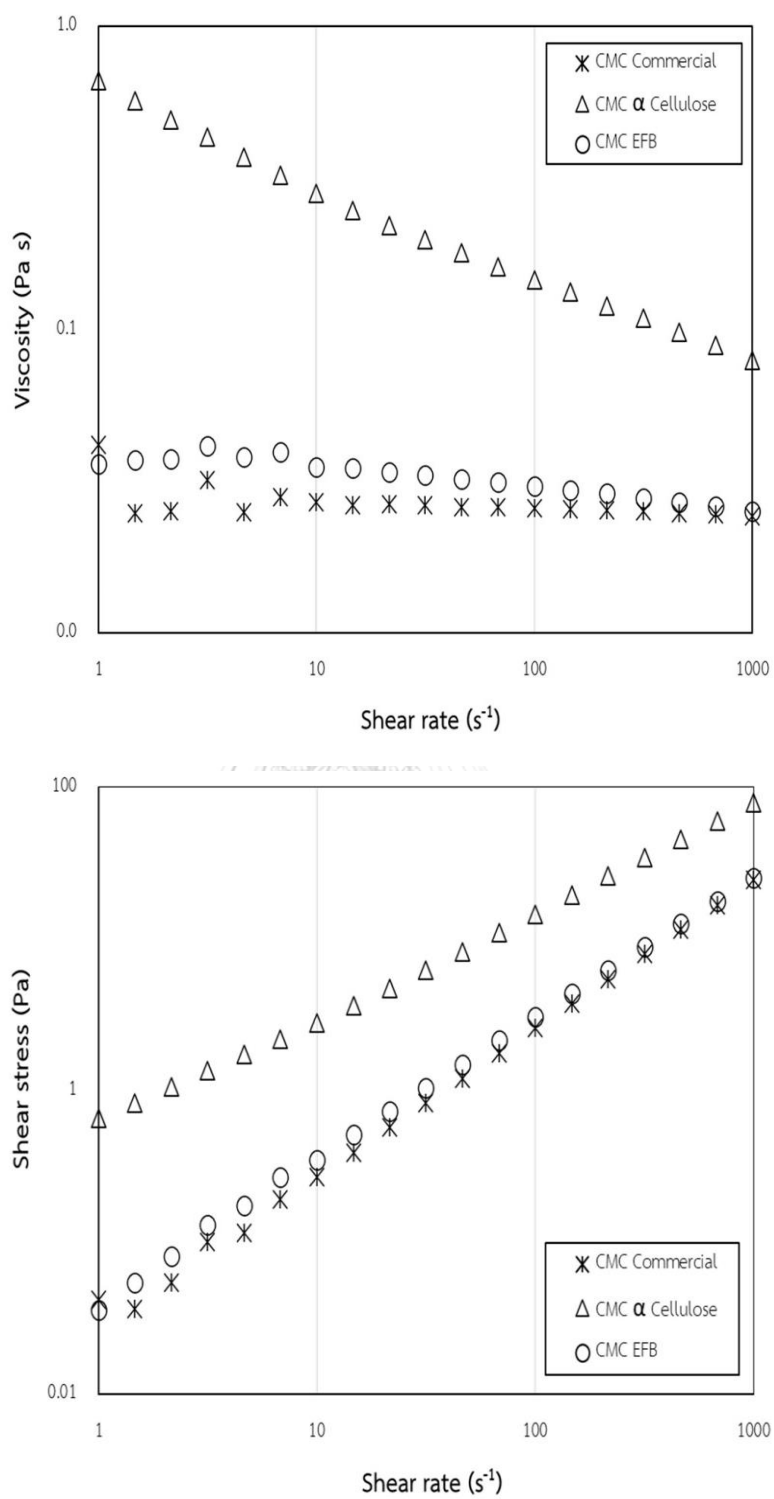
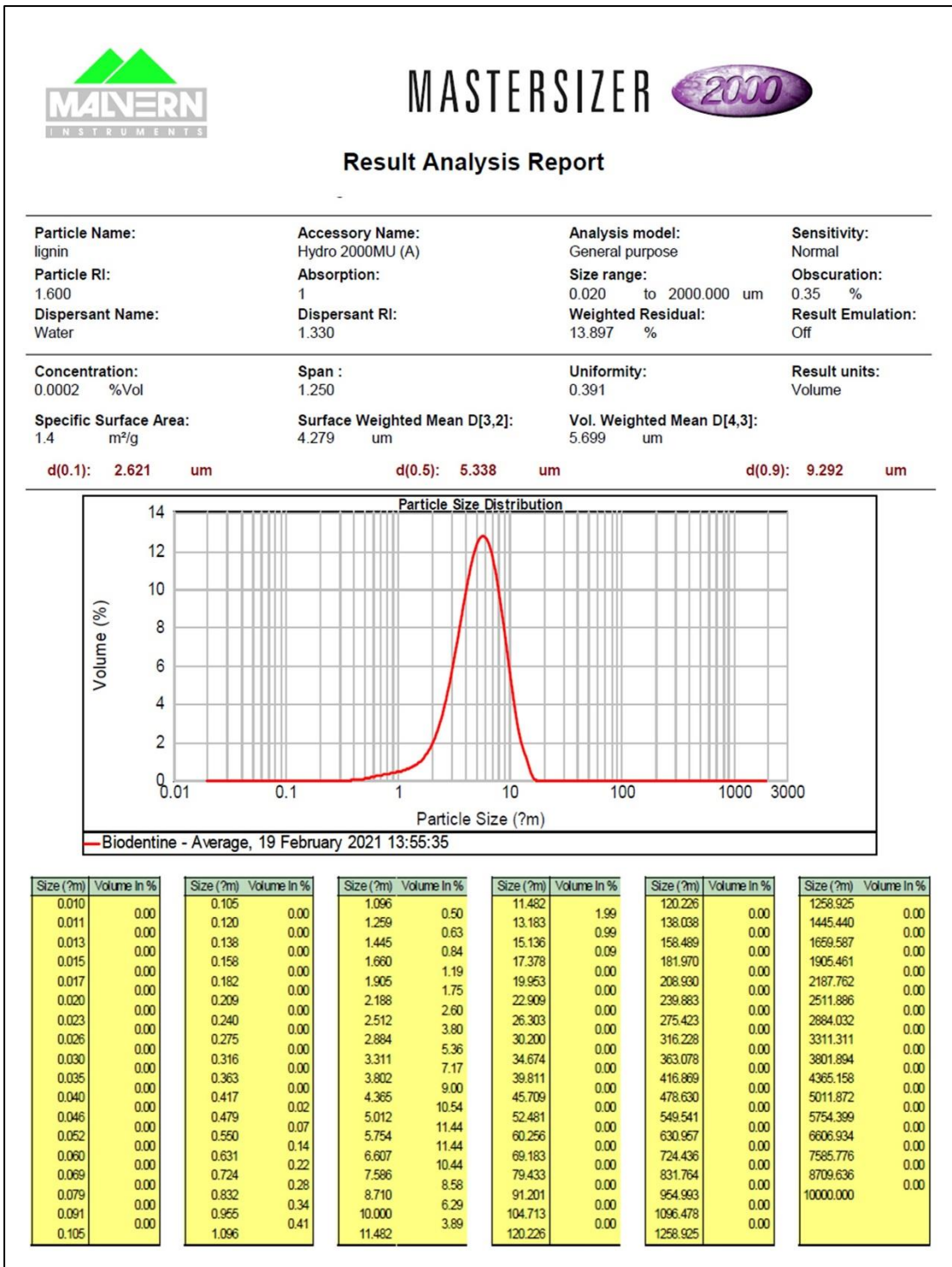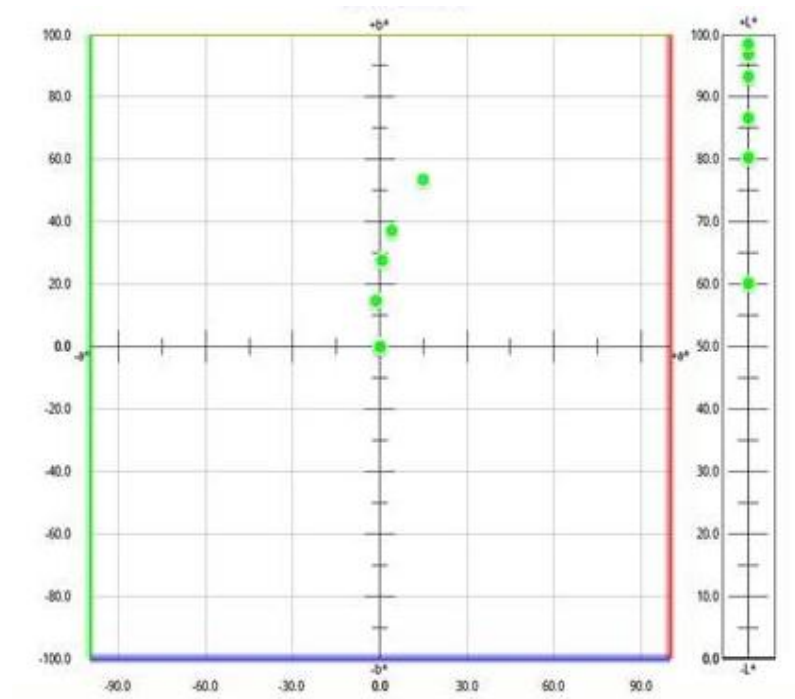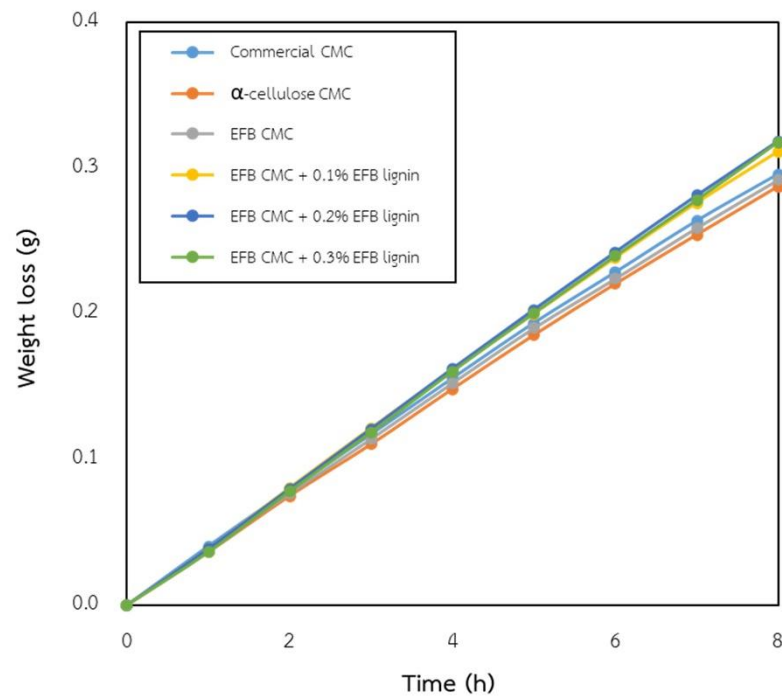**Figure A3** Rheological behavior of CMC-based films.

Figure A4 Results of EFB lignin particle size measurement.

Figure A5 Color diagram of all CMC-based composite film showing an increase in yellow and red due to increased EFB lignin concentration.

Figure A6 Linear regression of weight loss vs time (r^2 = 0.99) in the measurement of water vapor permeability.

VITA

NAME   Muhammad Taufiq Haqiqi

DATE OF BIRTH   22 February 1994

PLACE OF BIRTH   Kediri

INSTITUTIONS ATTENDED   Mulawarman University

HOME ADDRESS   Jl. P. Suryanata No.15, Kelurahan Bukit Pinang, Samarinda
                         75131, East Kalimantan, Indonesia.

PUBLICATION   Haqiqi, M.T., Bankeeree, W., Lotrakul, P., Pattananuwat, P.,
                         Punnapayak, H., Ramadhan, R., Kobayashi, T., Amirta, R.
                         and Prasongsuk, S. 2021. Antioxidant and UV-blocking
                         properties of a carboxymethyl cellulose-lignin composite
                         film produced from oil palm empty fruit bunch. ACS
                         Omega, 6(14): 9653-9666.

AWARD RECEIVED   The ASEAN scholarship, the global academia-industry
                         consortium for collaborative education (GAICCE) research
                         exchange scholarship program from AUN/SEED-Net, JICA,
                         the Sci-Super VI fund, the teaching assistant scholarship,
                         the COVID-19 student grant, and oral presentation at the
                         GAICCE International Symposium 2020.